

# Selective C–C Bond Formation between Alkynes Mediated by the $[\text{RuCp}(\text{PR}_3)]^+$ Fragment Leading to Allyl, Butadienyl, and Allenyl Carbene Complexes—An Experimental and Theoretical Study

Eva Rüba,<sup>[a]</sup> Kurt Mereiter,<sup>[b]</sup> Roland Schmid,<sup>[a]</sup> Valentin N. Sapunov,<sup>[a]</sup> Karl Kirchner,<sup>\*,[a]</sup> Herwig Schottenberger,<sup>[c]</sup> Maria José Calhorda,<sup>\*,[d]</sup> and Luis F. Veiros<sup>[e]</sup>

**Abstract:** The reaction of alkynes with  $[\text{RuCp}(\text{PR}_3)(\text{CH}_3\text{CN})_2]\text{PF}_6$  ( $\text{R} = \text{Me}, \text{Ph}, \text{Cy}$ ) affords, depending on the structure of the alkyne and the substituent of the phosphine ligand, allyl carbene or butadienyl carbene complexes. These reactions involve the migration of the phosphine ligand or a facile 1,2 hydrogen shift. Both reactions proceed via a metallacyclopentatriene complex. If no  $\alpha\text{C-H}$  bonds are accessible, allyl carbenes are formed, while in the presence of  $\alpha\text{C-H}$  bonds butadienyl carbenes are typically obtained. With diphenylacetylene, on the other hand, a cyclobutadiene complex is formed. A different reaction pathway is encountered with  $\text{HC}\equiv\text{CSiMe}_3$ , ethynylferrocene ( $\text{HC}\equiv\text{CFc}$ ),

and ethynylruthenocene ( $\text{HC}\equiv\text{CRc}$ ). Whereas the reaction of  $[\text{RuCp}(\text{PR}_3)(\text{CH}_3\text{CN})_2]\text{PF}_6$  ( $\text{R} = \text{Ph}$  and  $\text{Cy}$ ) with  $\text{HC}\equiv\text{CSiMe}_3$  affords a vinylidene complex, with  $\text{HC}\equiv\text{CFc}$  and  $\text{HC}\equiv\text{CRc}$  this reaction does not stop at the vinylidene stage but subsequent cycloaddition yields allenyl carbene complexes. This latter C–C bond formation is effected by strong electronic coupling of the metallocene moiety with the conjugated allenyl carbene unit, which facilitates

transient vinylidene formation with subsequent alkyne insertion into the  $\text{Ru}=\text{C}$  bond. The vinylidene intermediate appears only in the presence of bulky substituents of the phosphine coligand. For the small  $\text{R} = \text{Me}$ , head-to-tail coupling between two alkyne molecules involving phosphine migration is preferred, giving the more usual allyl carbene complexes. X-ray structures of representative complexes are presented. A reasonable mechanism for the formation of both allyl and allenyl carbenes has been established by means of DFT calculations. During the formation of allyl and allenyl carbenes, metallacyclopentatriene and vinylidene complexes, respectively, are crucial intermediates.

**Keywords:** alkynes • carbene complexes • density functional calculations • ruthenium • metallacyclopentatriene complexes

## Introduction

For some time we have probed the possibility of using ruthenium complexes for mediating the cyclotrimerization of alkynes. The metal compound envisaged for this purpose must bear at least two vacant coordination sites or, equivalently, two substitution-labile ligands. This is the case with  $[\text{RuCp}(\text{cod})\text{X}]$  and  $[\text{RuCp}^*(\text{cod})\text{X}]$  ( $\text{X} = \text{Cl}, \text{Br}$ ;  $\text{cod} = 1,5\text{-cyclo-octadiene}$ ), which have recently been shown to catalyze efficiently the cyclotrimerization of 1,6-diynes in combination with other alkynes.<sup>[1]</sup> We have used the substitutionally labile complex  $[\text{RuCp}(\text{PR}_3)(\text{CH}_3\text{CN})_2]\text{PF}_6$  ( $\text{R} = \text{Me}$  (**1a**),  $\text{Ph}$  (**1b**),  $\text{Cy}$  (**1c**)),<sup>[2]</sup> which features the synthetic equivalent of the 14-electron fragment  $[\text{RuCp}(\text{PR}_3)]^+$ . This entity is a promising candidate since it is possible to vary the ligand through its phosphine substituents. In this way the regioselectivity of the coupling process may be controlled. However, although **1** is catalytically active in the isomerization of allyl alcohols<sup>[3]</sup> and is a precatalyst for the transfer hydrogenation of acetophenone and cyclohexanone as well as the isomerization of allyl ethers,<sup>[4]</sup> cyclotrimerizations of alkynes were not initiated.

Instead, the reaction of **1** with alkynes leads to the formation of a number of unusual and intriguing products

[a] Prof. Dr. K. Kirchner, Dr. E. Rüba, Prof. Dr. R. Schmid, Prof. Dr. V.N. Sapunov  
Institute of Applied Synthetic Chemistry  
Vienna University of Technology  
Getreidemarkt 9, 1060 Vienna (Austria)  
Fax: (+43) 1-58801-15499  
E-mail: kkirch@mail.zserv.tuwien.ac.at

[b] Prof. Dr. K. Mereiter  
Institute of Chemical Technologies and Analytics  
Vienna University of Technology  
Getreidemarkt 9, 1060 Vienna (Austria)

[c] Prof. Dr. H. Schottenberger  
Institute of General, Inorganic, and Theoretical Chemistry  
University of Innsbruck  
Innrain 52a, 6020 Innsbruck (Austria)

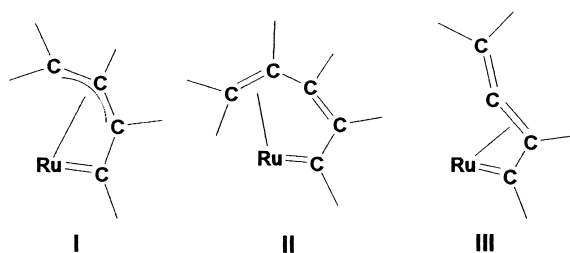
[d] Prof. Dr. M. J. Calhorda  
ITQB, Av. da República, EAN, Apart. 127, 2781-901 Oeiras, Portugal  
Departamento de Química e Bioquímica  
Faculdade de Ciências  
Universidade de Lisboa, 1749-016 Lisboa (Portugal)

[e] Prof. Dr. L. F. Veiros  
Centro de Química Estrutural  
Instituto Superior Técnico  
1049-001 Lisboa (Portugal)



Supporting information for this article is available on the WWW under <http://www.chemeurj.org/> or from the author.

involving ruthenium allyl carbene (**I**),<sup>[5]</sup> butadienyl carbene (**II**),<sup>[6]</sup> and allenyl carbene complexes (**III**),<sup>[7]</sup> depending on the structure of the alkyne and the substituent on the phosphine ligand. It is reasonable to speculate that there is a common



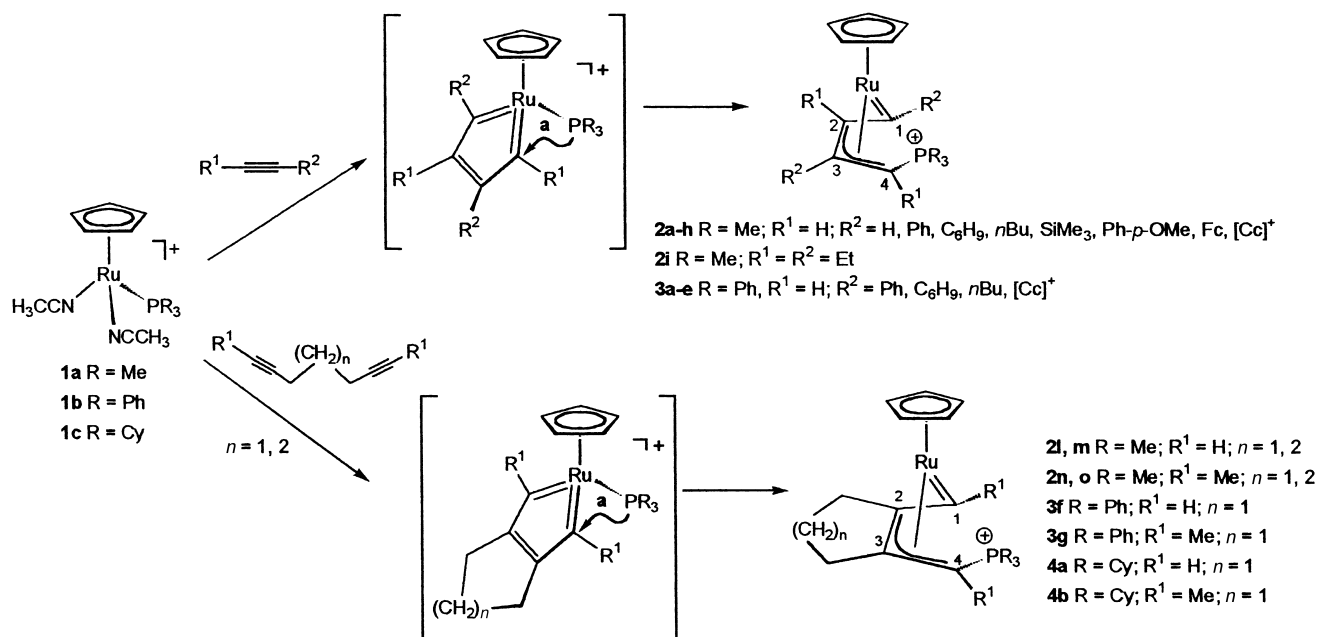
first step in the formation of allyl and butadienyl carbenes, which represents the formation of a highly electrophilic cationic metallacyclopentatriene complex as a result of oxidative coupling. In one case, such a complex could even be isolated (when the alkyne was deca-2,8-diyne and the phosphine in **1** was PCy<sub>3</sub>).<sup>[6]</sup> A key feature of the metallacyclopentatriene complexes appears to be the nucleophilicity of the coligand initiating phosphine migrations to give allyl carbenes, and the presence of  $\alpha$ -alkyl substituents favoring a 1,2-hydrogen shift to give butadienyl carbenes. In the particular case of using ethynylferrocene, an  $\eta^2$ -allenyl carbene complex is formed via a vinylidene intermediate. This is likely to be a result of efficient electronic coupling of the ferrocenyl moiety with the conjugated allenyl carbene unit. All these unexpected and unprecedented reactions actually quench the catalytic activity towards cyclotrimerization.

Notwithstanding this, metallacyclopentatriene complexes featuring the cyclic biscarbene structure are fascinating entities and appear to be important intermediates in various transformations of unsaturated organic molecules.<sup>[1, 8, 9]</sup> In general, however, the involvement of metallacyclopentatriene

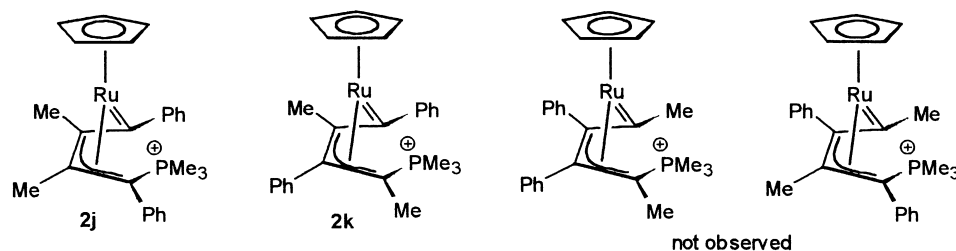
complexes is mere speculation since to date only a few actual examples are known.<sup>[10]</sup> From this point of view it is worthwhile to investigate the reactions of **1** described above. First, we will use further terminal and internal alkynes and diynes to synthesize several species featuring a Ru=C bond including metallacyclopentatrienes, allyl, butadienyl, and allenyl carbenes as well as vinylidene complexes. In this way we hope to be able to identify some intermediates more clearly and to obtain further information as to the underlying reaction mechanisms. For this reason, DFT calculations<sup>[11]</sup> will be performed to support the interpretations of the experimental results. In addition, X-ray structures of representative complexes will be presented.

## Results and Discussion

**Synthesis of allyl and butadienyl carbenes:** The complexes **1a–c** were allowed to react with one or two equivalents of the following types of alkynes: terminal alkynes HC≡CR<sup>1</sup> (R<sup>1</sup> = H, Ph, C<sub>6</sub>H<sub>9</sub>, *n*Bu, SiMe<sub>3</sub>, Ph-*p*-OMe, ferrocenyl (Fc), cobaltocenium hexafluorophosphate (Cc<sup>+</sup>)), internal alkynes R<sup>1</sup>C≡CR<sup>2</sup> (R<sup>1</sup> = R<sup>2</sup> = Et and R<sup>1</sup> = Me, R<sup>2</sup> = Ph), and diynes R<sup>1</sup>C≡CCH<sub>2</sub>(CH<sub>2</sub>)<sub>*n*</sub>CH<sub>2</sub>C≡CR<sup>2</sup> (R<sup>1</sup> = R<sup>2</sup> = H, Me; *n* = 1, 2). Throughout,  $\eta^3$ -allyl carbene complexes (**2a–o**, **3a–f**, **4a**) were obtained in high yields according to Scheme 1. Most of these reactions are fast even at room temperature and are completed within a few minutes, as may be monitored by NMR spectroscopy. The identity of the compounds was established by <sup>1</sup>H, <sup>13</sup>C{<sup>1</sup>H}, and <sup>31</sup>P{<sup>1</sup>H} NMR spectroscopy, and usually also by elemental analysis. With terminal alkynes no isomers were obtained and C–C coupling was highly selective in a head-to-tail fashion with the substituents ending up in the 1- and 3-positions. However, the asymmetric alkyne MeC≡CPh resulted in the formation of two isomeric allyl carbenes **2j** and **2k** in a 10:7 ratio. Note that there was no



Scheme 1. The preparation of  $\eta^3$ -allyl carbene complexes from R<sup>1</sup>C≡CCH<sub>2</sub>(CH<sub>2</sub>)<sub>*n*</sub>CH<sub>2</sub>C≡CR<sup>2</sup> (R<sup>1</sup> = R<sup>2</sup> = H, Me; *n* = 1, 2).

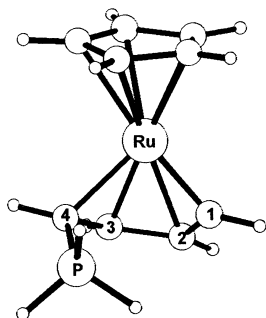


evidence for an isomer with two phenyl substituents in the 2,3-positions. Moreover, no isomer with a methyl group attached to the carbene carbon atom is formed. The slight favoring of **2j** over **2k** may be due to steric reasons such as the repulsive interactions between methyl and phenyl groups which are less pronounced in the C–C bond-forming oxidative coupling step than between two phenyl groups (cf. cone angles: Me: 90°; Ph: 105°<sup>[12]</sup>).

The <sup>13</sup>C{<sup>1</sup>H} NMR spectra of the  $\eta^3$ -allyl carbene complexes exhibit a characteristic low-field doublet resonance in the range  $\delta = 279$ –236 ppm ( $J_{C,P} = 3$ –7 Hz) and a doublet in the range  $\delta = 41$ –26 ppm ( $J_{C,P} = 66$ –77 Hz) which may be assigned to the carbene carbon atom C1 and the terminal allyl carbon atom C4 bearing the phosphine substituent. Furthermore, the <sup>1</sup>H NMR spectra of **2a**, **2l**, **2m**, **3a**, **3f**, and **4a** exhibit a very characteristic low-field resonance of the carbene hydrogen atom H1 between  $\delta = 12.4$  and 11.4 ppm.

The structures of **2b**, **2g**, **3g**, and **4b** obtained from X-ray crystallography are shown in Figures 1–4, and selected bond lengths and angles are summarized in Table 1.

Table 1. Selected bond lengths [Å] and angles [°] of some allyl carbene complexes and comparison with the DFT/B3LYP-optimized<sup>[a]</sup> structure of [CpRu(=CH- $\eta^3$ -CHCHCHPH<sub>3</sub>)]<sup>+</sup>.



|                     | <b>2b</b> | <b>2l</b> <sup>[b]</sup> | <b>2g</b> | <b>3g</b> · ½CH <sub>2</sub> Cl <sub>2</sub> | <b>4b</b> | Calcd |
|---------------------|-----------|--------------------------|-----------|--|-----------|-------|
| Ru–C1               | 1.908(2)  | 1.897(2)                 | 1.916(6)  | 1.898(4)                                     | 1.903(3)  | 1.911 |
| Ru–C2               | 2.205(2)  | 2.232(2)                 | 2.201(6)  | 2.179(4)                                     | 2.191(3)  | 2.267 |
| Ru–C3               | 2.169(2)  | 2.174(2)                 | 2.187(6)  | 2.151(4)                                     | 2.147(3)  | 2.199 |
| Ru–C4               | 2.135(2)  | 2.123(2)                 | 2.141(7)  | 2.162(4)                                     | 2.189(3)  | 2.146 |
| C1–C2               | 1.410(3)  | 1.403(3)                 | 1.388(8)  | 1.415(6)                                     | 1.488(4)  | 1.414 |
| C2–C3               | 1.430(3)  | 1.426(3)                 | 1.421(8)  | 1.425(6)                                     | 1.424(3)  | 1.429 |
| C3–C4               | 1.448(3)  | 1.432(3)                 | 1.431(8)  | 1.434(6)                                     | 1.440(3)  | 1.449 |
| C4–P                | 1.774(2)  | 1.778(2)                 | 1.781(6)  | 1.799(4)                                     | 1.826(2)  | 1.783 |
| Ru–C <sub>pav</sub> | 2.209(3)  | 2.221(3)                 | 2.189(6)  | 2.206(7)                                     | 2.212(4)  | 2.269 |
| C1–C2–C3            | 117.0(2)  | 116.3(1)                 | 118.3(6)  | 117.4(4)                                     | 117.9(2)  | 115.5 |
| C2–C3–C4            | 118.9(2)  | 122.0(1)                 | 119.9(6)  | 122.5(4)                                     | 122.2(2)  | 120.7 |
| C3–C4–P             | 126.6(2)  | 125.4(1)                 | 126.1(5)  | 123.3(4)                                     | 120.6(1)  | 121.4 |
| C1–C2–C3–C4         | –16.8(4)  | –16.6(3)                 | –14.4(9)  | –15.5(6)                                     | –20.0(3)  | –19.7 |

[a] B3LYP Ru: sdd; C, H, P: 6–31g\*\*. [b] Ref. [5].

These results clearly reveal that in the case of terminal alkynes, C–C coupling had occurred between the internal and terminal sp-carbon atoms with the substituents ending up on the carbene carbon atom and the internal carbon atom of the allylic moiety, whereas with the diynes, the two internal sp-carbon atoms are involved.

In the allyl carbene systems formed, all four carbon atoms of the C1–C4 chain are bonded to the RuCp fragment in both cases. The C1–C4 chain is nearly planar; the torsion angles lie between  $-14.4$  and  $-20.0^\circ$ . The very short Ru–C1 bond (1.897–1.916 Å) is further evidence that C1 is an alkylidene carbon atom doubly bonded to the ruthenium center. The remaining three carbon atoms of the

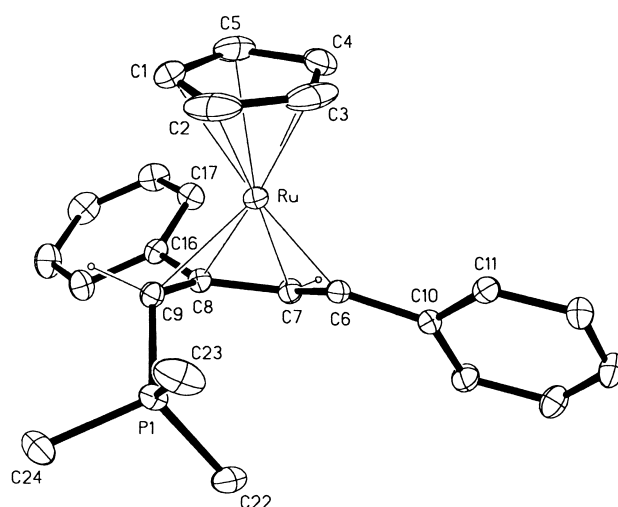


Figure 1. Structure of **2b** (20% thermal ellipsoids; PF<sub>6</sub><sup>–</sup> omitted for clarity).

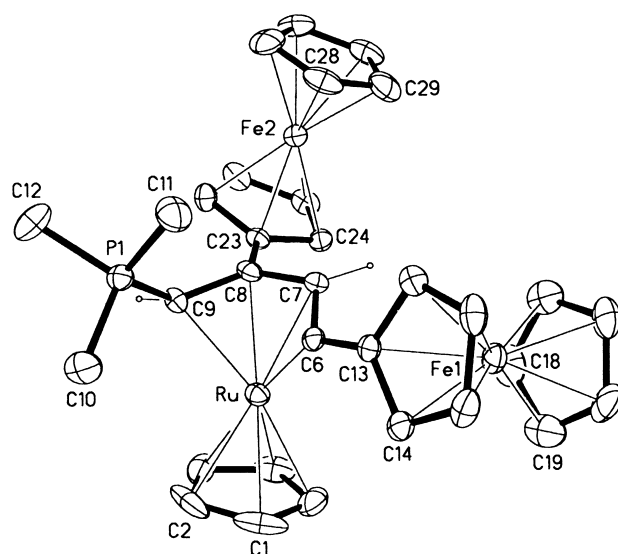


Figure 2. Structure of **2g** (20% thermal ellipsoids; PF<sub>6</sub><sup>–</sup> omitted for clarity).

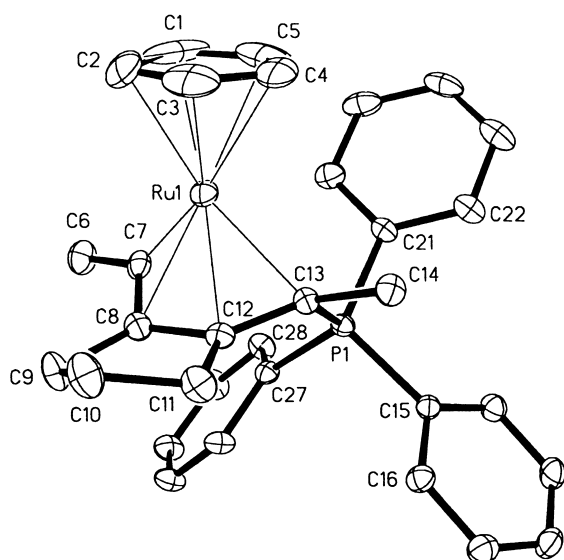


Figure 3. Structure of **3g**·½CH<sub>2</sub>Cl<sub>2</sub> (20% thermal ellipsoids; PF<sub>6</sub><sup>−</sup> and CH<sub>2</sub>Cl<sub>2</sub> omitted for clarity).

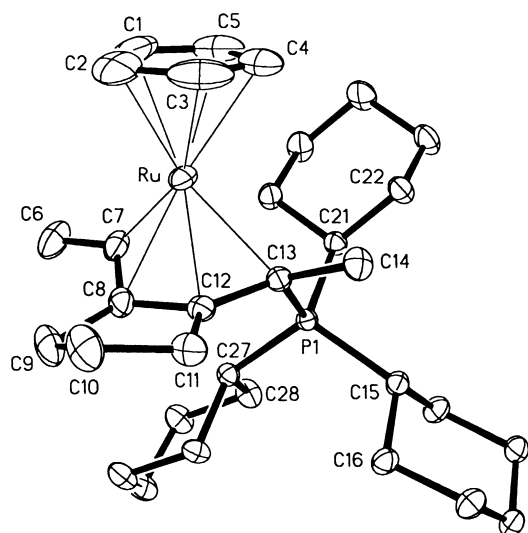


Figure 4. Structure of **4b** (20% thermal ellipsoids; PF<sub>6</sub><sup>−</sup> omitted for clarity).

C2–C4 chain have C–C distances that are typical of the  $\eta^3$ -allyl system. Owing to the near planarity of the C1–C4 chain, the  $\pi$  system of the allyl unit is capable of interacting with the Ru=C  $\pi$  bond with the consequence that the C–C distances within the allyl carbene moiety are relatively uniform. On the other hand, the unusual high-field shift of C4 may indicate substantial  $sp^3$  character of this atom requiring a major contribution from a ruthenacyclopenta-1,3-diene resonance structure.<sup>[13]</sup>

A different reaction takes place when **1a** is treated with PhC≡CPh. Whereas at room temperature no reaction occurs at all, at 80 °C the cationic  $\eta^4$ -cyclobutadiene complex [RuCp( $\eta^4$ -C<sub>4</sub>Ph<sub>4</sub>)(PMe<sub>3</sub>)]<sup>+</sup> (**5**) forms rather than an allyl carbene (Scheme 2). Complex **5** was fully characterized by NMR spectroscopy, elemental analysis, and X-ray crystallography. A structural view of **5** is shown in Figure 5. This is in

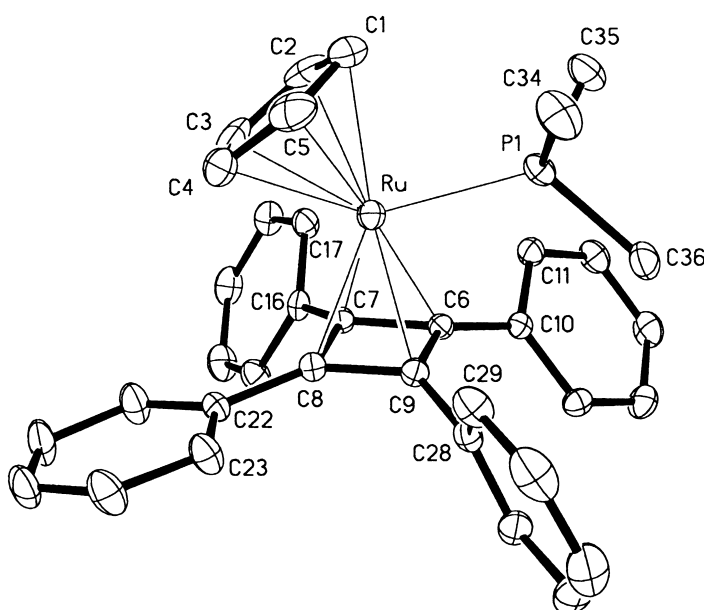
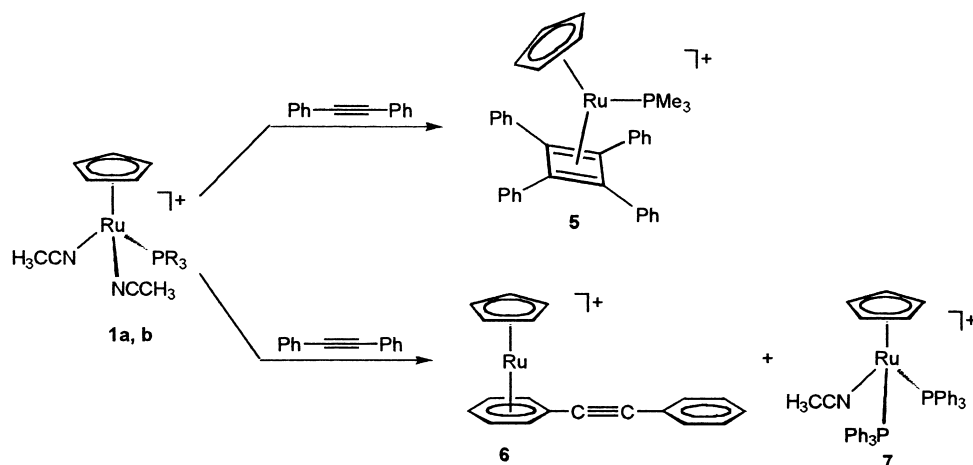


Figure 5. Structure of **5** (20% thermal ellipsoids; PF<sub>6</sub><sup>−</sup> omitted for clarity). Selected bond lengths [Å]: Ru–C<sub>pav</sub> 2.227(6), Ru–C6 2.172(4), Ru–C7 2.173(4), Ru–C8 2.191(5), Ru–C9 2.162(5), Ru–P1 2.382(2), C6–C7 1.444(6), C6–C9 1.515(6), C7–C8 1.481(6), C8–C9 1.438(6).



Scheme 2. The preparation of **5** from **1a** and **6** and **7** from **1b**.

line with work by Green and co-workers<sup>[14]</sup> according to which the dimeric complex  $[\{\text{RuCp}(\text{CO})_2\}_2]$  also reacts with  $\text{PhC}\equiv\text{CPh}$  in the presence of  $\text{Ag}^+$  at room temperature to give, in addition to bis- and tris-carbonyl  $\text{RuCp}$  complexes, the related  $\eta^4$ -cyclobutadiene complex  $[\text{RuCp}(\eta^4\text{-C}_4\text{Ph}_4)(\text{CO})]^+$ . Although the formation of a  $\eta^4$ -cyclobutadiene complex is thermodynamically favorable on the basis of DFT calculations (see below, structure **F** in Figure 7) it is apparently kinetically unfavorable.

In contrast to **1a**, complex **1b** reacts with  $\text{PhC}\equiv\text{CPh}$  at  $80^\circ\text{C}$  to give quantitatively the known sandwich complex  $[\text{RuCp}(\eta^6\text{-C}_6\text{H}_5\text{-C}\equiv\text{CPh})]^+$  (**6**)<sup>[15, 16]</sup> together with the known bisphosphine complex  $[\text{RuCp}(\text{PPh}_3)_2(\text{CH}_3\text{CN})]^+$  (**7**)<sup>[17]</sup> in a 1:1 ratio (Scheme 2). There was no evidence of the occurrence of an allyl carbene or a cyclobutadiene species. With **1c**, on the other hand, no clean reaction took place and several intractable materials, together with small amounts of **6**, were formed.

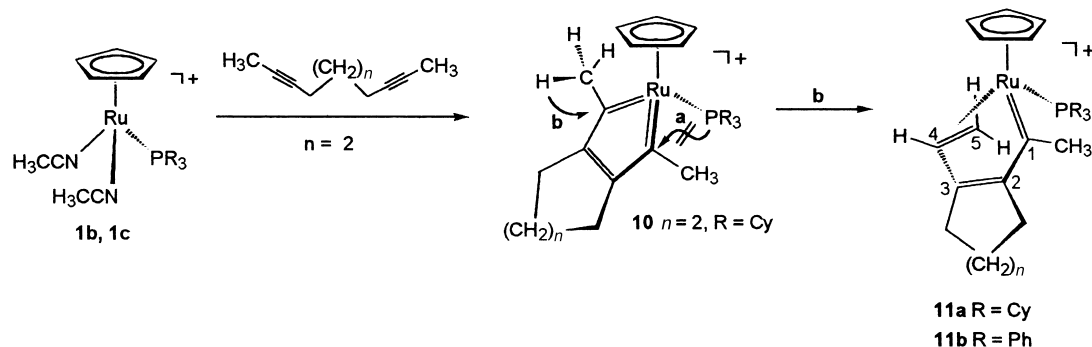
Although with the formation of the allyl carbenes no intermediates could be detected spectroscopically, it is reasonable to suggest the involvement of a metallacyclopentatriene intermediate as the result of oxidative coupling (Scheme 1). In one case, namely the reaction of **1c** with 2,8-decadiyne, such an intermediate has been observed by  $^1\text{H}$ ,  $^{13}\text{C}\{^1\text{H}\}$ , and  $^{31}\text{P}\{^1\text{H}\}$  NMR spectroscopy. The resonances in the  $^{13}\text{C}\{^1\text{H}\}$  NMR spectrum at  $\delta = 325.6$  and  $170.6$  ppm can be associated with the  $\text{C}_\alpha$  and  $\text{C}_\beta$  ring carbon atoms, respectively. In addition, the unusual down-field shift of the  $\text{C}_\alpha$ -carbon resonance is in agreement with an unsaturated bis-carbene ligand. Thus the formation of the cationic metallacyclopentatriene structure  $[\text{CpRu}(\text{=C}_2(\text{CH}_3)_2\text{C}_2(\text{CH}_2)_4)(\text{PCy}_3)]^+$  (**10**) (Scheme 3) is indicated. In a similar fashion, as shown recently,<sup>[18]</sup> the complex  $[\text{RuCp}(\text{SbPh}_3)(\text{CH}_3\text{CN})_2]\text{PF}_6$  reacts with 2,8-decadiyne to afford the analogous cationic metallacyclopentatriene complex  $[\text{CpRu}(\text{=C}(\text{CH}_3)_2\text{C}_2(\text{CH}_2)_4)(\text{SbPh}_3)]^+$ . The latter also exhibits characteristic resonances in the  $^{13}\text{C}\{^1\text{H}\}$  NMR spectrum at  $\delta = 330.3$  and  $171.3$  ppm, which are assigned to the  $\text{C}_\alpha$  and  $\text{C}_\beta$  ring carbon atoms, respectively (cf. the neutral metallacyclopentatriene  $[\text{RuCp}(\text{=C}_2(\text{Ph})_2\text{CH}_2)\text{Br}]$ , for which the respective resonances of the  $\text{C}_\alpha$  and  $\text{C}_\beta$  atoms occur at  $\delta = 271.1$  and  $156.0$  ppm<sup>[10a]</sup>). The metallacyclopentatriene complex **10**, however, is unstable and converts directly into the butadienyl carbene complex  $[\text{CpRu}(\text{=C}(\text{CH}_3)\text{C}(\text{CH}_2)_4\text{C-}\eta^2\text{-CH=CH}_2)(\text{PCy}_3)]\text{PF}_6$  (**11a**). The step from **10** to **11a** involves activation of an  $\alpha$ -substituent by one of the electrophilic carbene carbon atoms.

This is formally a 1,2-hydrogen shift which is unprecedented for a metallacyclopentatriene. There is only one more example of a butadienyl carbene as encountered recently in the reaction of an osmacyclopentatriene complex with *tert*-butylamine.<sup>[19]</sup> Likewise, the analogous butadienyl carbene **11b** is formed by the reaction of **1b** with 2,8-decadiyne, again without any intermediate being observed.

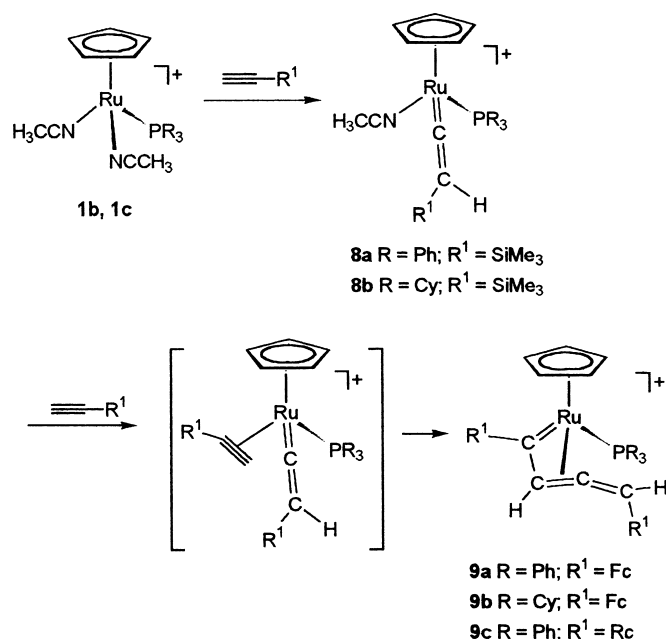
Both types of reactions described above, attack of a nucleophile onto a carbene carbon atom (phosphine ligand) and a 1,2-hydrogen shift, are typical of very electrophilic, usually cationic, carbenes.<sup>[20]</sup> This is further support for our proposal that a metallacyclopentatriene is a key intermediate in the formation of allyl and butadienyl carbenes. A feasible low-energy pathway to give allyl carbenes via a metallacyclopentatriene species follows from DFT calculations (vide infra).

**Synthesis of allenyl carbenes:** A completely different type of reaction is encountered when the alkynes  $\text{HC}\equiv\text{CSiMe}_3$ , ethynylferrocene ( $\text{HC}\equiv\text{CFc}$ ), and ethynylruthenocene ( $\text{HC}\equiv\text{CRc}$ ) are allowed to react with either **1b** or **1c**. While **1a** undergoes the expected reaction with  $\text{HC}\equiv\text{CSiMe}_3$  to yield the allyl carbene **2e**, both **1b** and **1c** afford the cationic vinylidene complexes  $[\text{CpRu}(\text{=C=CHSiMe}_3)(\text{CH}_3\text{CN})(\text{PPh}_3)]^+$  (**8a**) and  $[\text{CpRu}(\text{=C=CHSiMe}_3)(\text{CH}_3\text{CN})(\text{PCy}_3)]^+$  (**8b**) in quantitative yield as monitored by NMR spectroscopy (Scheme 4). Unfortunately, neither **8a** nor **8b** could be isolated in pure form due to the formation of several intractable decomposition compounds upon work-up. Characteristic features comprise, in the  $^{13}\text{C}\{^1\text{H}\}$  NMR spectrum, a marked low-field resonance at  $\delta = 321.3$  (d,  $J_{\text{C,P}} = 17.3$  Hz) and  $320.5$  ppm (d,  $J_{\text{C,P}} = 15.4$  Hz), respectively, which may be assigned to the  $\alpha$ -carbon atom of the vinylidene moiety. The  $\text{C}_\beta$  atom displays a resonance at  $\delta = 100.1$  and  $100.2$  ppm, respectively. Furthermore, the  $\text{C}_\beta$ -hydrogen atom shows a doublet centered at  $\delta = 3.93$  ( $J_{\text{C,P}} = 4.0$  Hz) and  $4.06$  ppm ( $J_{\text{C,P}} = 2.5$  Hz), respectively.  $^{31}\text{P}\{^1\text{H}\}$  NMR resonances are observed at  $53.7$  and  $59.0$  ppm, respectively.

When complexes of **1** are treated with ethynylferrocene ( $\text{HC}\equiv\text{CFc}$ ), where the ferrocenyl unit is bonded directly to the alkynyl group, only **1a** yields the  $\eta^3$ -allyl carbene complex  $[\text{CpRu}(\text{=C}(\text{Fc})\text{-}\eta^3\text{-CHC}(\text{Fc})\text{CHPMe}_3)]\text{PF}_6$  (**2g**). In the other cases (**1b** or **1c**) the novel  $\eta^2$ -allenyl carbene complexes  $[\text{CpRu}(\text{=C}(\text{Fc})\text{-}\eta^2\text{-CH=C=CH}(\text{Fc}))(\text{PPh}_3)]\text{PF}_6$  (**9a**) and  $[\text{CpRu}(\text{=C}(\text{Fc})\text{-}\eta^2\text{-CH=C=CH}(\text{Fc}))(\text{PCy}_3)]\text{PF}_6$  (**9b**) are formed



Scheme 3. The formation of unstable complex **10**, which rearranges to give **11**.

Scheme 4. The formation of **8a, b** and **9a–c**.

in 65 and 71 % yield, respectively (see Scheme 4).<sup>[7]</sup> The analogous allenyl carbene  $[\text{CpRu}(\text{=C}(\text{Rc})\text{-}\eta^2\text{-CH=C=CH}(\text{Rc}))(\text{PPh}_3)]\text{PF}_6$  (**9c**) is obtained from **1b**, along with  $\text{HC}\equiv\text{CRc}$  (Rc = ruthenocenyl), with NMR spectroscopic features very similar to those of **9a** and **9b**. It should be mentioned that the isostructural and isoelectronic ethynyl cobaltocenium hexafluorophosphate ( $[\text{HC}\equiv\text{CCc}]\text{PF}_6$ ) reacts with **1a** to give an allyl carbene or, in the case of **1b**, its rearrangement product. More details will be given in a forthcoming paper.<sup>[21]</sup>

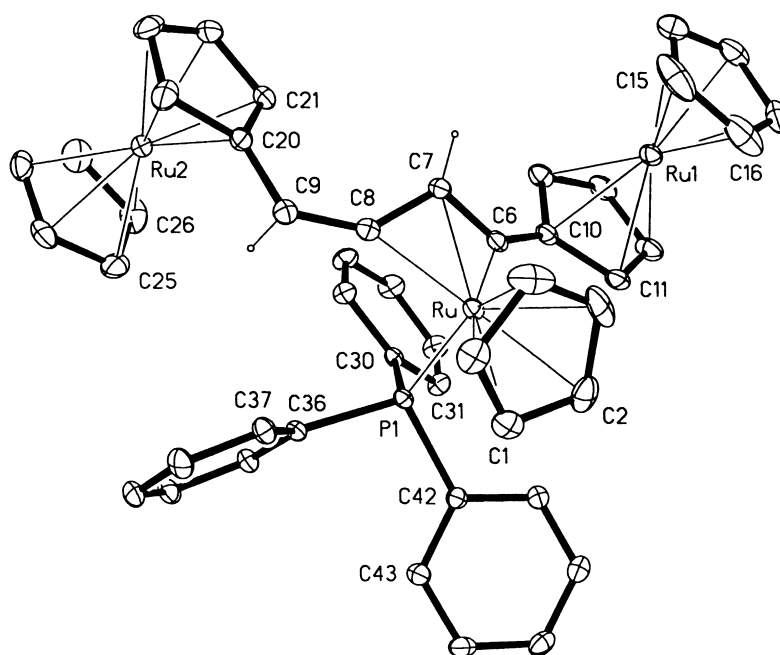
The molecular structure of **9c** (in form of the crystalline solvate **9c**·CH<sub>2</sub>Cl<sub>2</sub>) as confirmed by X-ray crystallography<sup>[22]</sup> is depicted in Figure 6, and selected bond lengths and angles of **9a** and **9c** are given in Table 2. The overall structure of **9c**·CH<sub>2</sub>Cl<sub>2</sub> is very similar to that of **9a**.<sup>[7]</sup> The most notable features are 1) the *exo* orientation of the C6–C7–C8 moiety with respect to the phosphine ligand, 2) the distorted *s-trans* structure of the C6–C7–C8–C9 unit, and 3) the short Ru–C6 bond length of 1.940(3) Å. The latter is characteristic of an alkylidene double-bonded to the ruthenium center. The two allenyl carbon atoms, C7 and C8, are noticeably further away from the Ru center and asymmetrically bonded (Ru–C7 2.168(3), Ru–C8 2.093(3) Å) while the terminal allenyl carbon atom, C9, is not coordinated to the metal center (Ru–C9

Table 2. Selected bond lengths [Å] and angles [°] of allenyl carbene complexes and comparison with the DFT/B3LYP-optimized<sup>[6]</sup> structure of  $[\text{CpRu}(\text{=CH-}\eta^2\text{-CH=C=CH}_2)(\text{PH}_3)]^+$ .

|                     | <b>9a</b> ·CH <sub>2</sub> Cl <sub>2</sub> <sup>[b]</sup> | <b>9c</b> ·CH <sub>2</sub> Cl <sub>2</sub> | Calcd  |
|---------------------|---|--|--------|
| Ru–C1               | 1.943(2)  | 1.940(3)                                   | 1.919  |
| Ru–C2               | 2.171(3)  | 2.168(3)                                   | 2.239  |
| Ru–C3               | 2.099(3)  | 2.093(3)                                   | 2.122  |
| Ru–P                | 2.322(1)  | 2.323(1)                                   | 2.323  |
| C1–C2               | 1.415(4)  | 1.415(5)                                   | 1.399  |
| C2–C3               | 1.416(4)  | 1.422(4)                                   | 1.430  |
| C3–C4               | 1.321(3)  | 1.322(5)                                   | 1.326  |
| Ru–Cp <sub>av</sub> | 2.233(3)  | 2.241(4)                                   | 2.287  |
| C1–C2–C3            | 116.3(2)  | 115.7(3)                                   | 115.8  |
| C2–C3–C4            | 138.0(3)  | 138.6(3)                                   | 140.0  |
| C1–C2–C3–C4         | –151.7(3)   | –151.2(4)                                  | –152.3 |

[a] B3LYP Ru: sdd; C, H, P: 6–31g\*\*. [b] Ref. [7].

3.281 Å). Whereas, therefore, **9** is best described as an  $\eta^2$ -allenyl carbene, a resonance contribution from the allylic structure is evident from the rather uniform bond lengths found for C6–C7 (1.415(4) Å) and C7–C8 (1.422(4) Å). Thus,  $\pi$ -electron delocalization appears to be substantial. The C8–C9 bond length of 1.322(5) Å is typical of a noncoordinated C=C bond. The C–C bond lengths linking the two ruthenocenyl moieties with the allenyl carbene C1–C4 unit

Figure 6. Structure of **9c**·½CH<sub>2</sub>Cl<sub>2</sub> (20 % thermal ellipsoids; PF<sub>6</sub><sup>–</sup> and CH<sub>2</sub>Cl<sub>2</sub> omitted for clarity).

are quite different from one another; C6–C10 = 1.404(5) Å and C9–C20 = 1.468(5) Å. In addition, the C–C bond lengths within the cyclopentadienyl ligand of the ruthenocenyl substituent attached to the carbene-carbon atom C6 are significantly different with C10–C11 and C10–C14 being longer (1.439(5) and 1.452(5) Å, respectively) and C11–C12, C12–C13, and C13–C14 being shorter (1.410(5), 1.414(6), and 1.409(5) Å, respectively). Thus a fulvene-like structure is adopted similarly to the ferrocenyl analogue **9a**.<sup>[7]</sup>

An appealing mechanism for the formation of  $\eta^2$ -allenyl carbene complexes is presented in Scheme 4. Accordingly, the first intermediate is the cationic vinylidene complex  $[\text{CpRu}(=\text{C}=\text{CHR}^1)(\text{CH}_3\text{CN})(\text{PR}_3)]^+$  as is actually observed in an analogous reaction using  $\text{HC}\equiv\text{CSiMe}_3$  as the alkyne. After subsequent replacement of the  $\text{CH}_3\text{CN}$  ligand by a second alkyne molecule to give an  $\eta^2$ -alkyne vinylidene species  $[\text{CpRu}(=\text{CHR}^1)(\eta^2\text{-HC}\equiv\text{CR}^1)(\text{PR}_3)]^+$ , the alkyne is inserted into the  $\text{Ru}=\text{C}$  bond. That this reaction series is restricted to the presence of bulky coligands could point to the importance of steric effects. It is well known that vinylidene formation is facilitated under such conditions.<sup>[23]</sup> However, another effect seems to be even more important since the ethynylcobaltocenium cation  $[\text{HC}\equiv\text{CCc}]^+$ , though isostructural and isoelectronic with ethynylferrocene and ethynylruthenocene, does not yield an allenyl carbene. Therefore,  $\pi$  conjugation of the C1–C4 chain of the allenyl carbene unit with one of the Cp  $\pi$  systems of the ferrocenyl and ruthenocenyl moieties likely favors this construction through the efficient stabilization of positive charge. This highlights the unique electronic properties of the ferrocenyl and ruthenocenyl fragments.

### Theoretical studies

**The bisacetylene precursor and the formation of allyl carbenes:** A general pathway for the conversion of the bisacetonitrile complex  $[\text{CpRu}(\text{NCH})_2(\text{PH}_3)]^+$  (**1**; the model with NCH and  $\text{PH}_3$  will be called **A**), into the allylcarbene species **2** and **3** (**E** when  $\text{R}^1 = \text{R}^2 = \text{H}$ ) is schematically shown in Figure 7 as a result of DFT/B3LYP<sup>[24]</sup> calculations using Gaussian98.<sup>[25]</sup> The reliability of the computational method

(details in Experimental Section) can be checked by comparing the calculated geometries of the final species (Figure 7) with X-ray structures available for complexes based on  $\text{PMe}_3$  (**2**) and on  $\text{PPh}_3$  (**3**) and several terminal acetylenes, or on  $\text{PCy}_3$  and diynes (**4**). Relevant data are given in Table 1.

The general agreement of calculated distances and angles with the experimental values is very good despite the absence of substituents in the model. A similarly good agreement is observed between the calculated structure of the initial complexes **1** (shown in Figure 7 as **A**) and the available X-ray structures (see Supporting Information, Table S1).

The first step in Figure 7 consists of the substitution of acetonitrile by acetylene, which is known experimentally to proceed by means of a dissociative mechanism,<sup>[2]</sup> leading to a monoacetonitrile complex. The associative alternative in which the coordination of acetylene is accompanied by  $\eta^5 \rightarrow \eta^3$  ring slippage to preserve the 18-electron count can be excluded. It may be noted that a dissociative pathway has also been proposed for the similar reaction of substitution of phosphine by acetylene in  $[\text{CpCo}(\text{PR}_3)_2]$ .<sup>[26]</sup> The thermodynamic profile for the substitution process is shown in Figure 8.

The high energy of the monoacetonitrile complex  $[\text{CpRu}(\text{NCH})(\text{PH}_3)]^+$  (**A1**) makes its formation appear to be the rate-limiting step of the overall reaction. The coordination of the first acetylene to the unsaturated **A1** to form **A2**

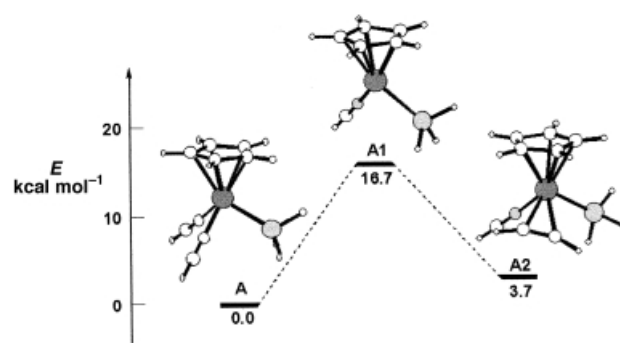


Figure 8. Profile of the B3LYP potential energy surface for the formation of monoacetylene complex **A2**.

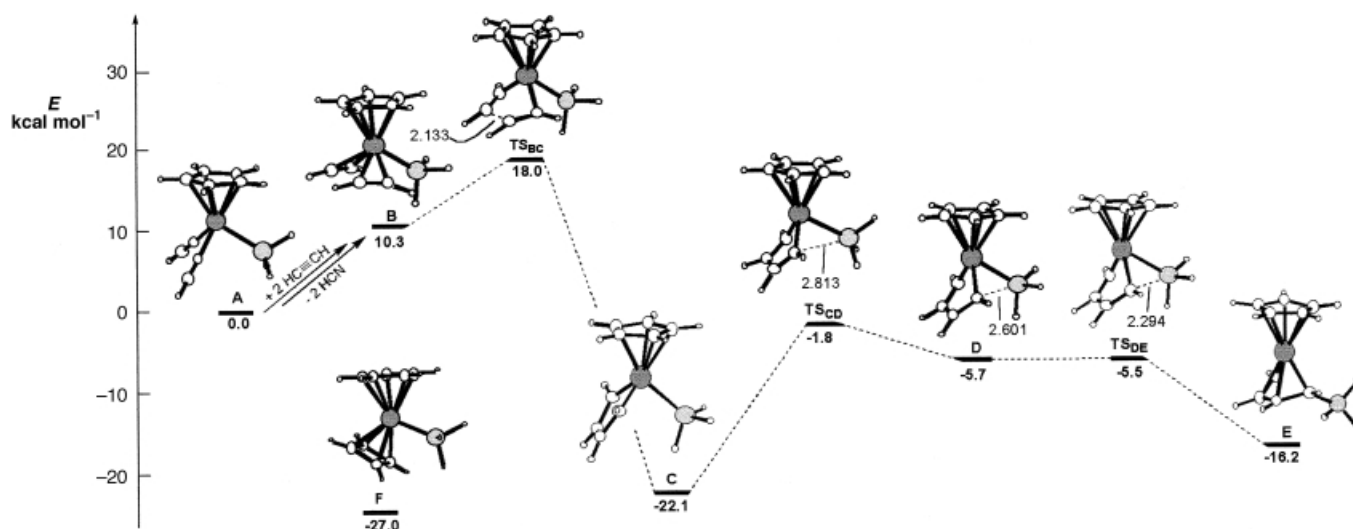


Figure 7. Profile of the B3LYP potential energy surfaces for the conversion of the bis-nitrile complex **A** into the allyl carbene **E**.

is exothermic by 13 kcal mol<sup>-1</sup>, but the acetylene complexes are higher in energy than the acetonitrile derivatives. The calculated energy differences between the proposed intermediates are of the order of magnitude of the activation barriers determined from NMR studies. Although transition states were not determined, their energies are not expected to be much higher than those of the unsaturated intermediates.

Bisacetylene complexes have been proposed as intermediates in several conversions such as in cyclotrimerizations, but no representative of Ru is known. For comparison purposes we use the bisacetylene complexes of Mo<sup>II</sup> of the type [CpMo( $\eta^2$ -R<sub>2</sub>C<sub>2</sub>)(L)]<sup>+</sup> (R = Me, L = I, CO, NCM<sub>2</sub>; R = Ph, L = CO), retrieved from the CSD.<sup>[27]</sup> The average C–C distance in [CpRu(C<sub>2</sub>H<sub>2</sub>)<sub>2</sub>(PH<sub>3</sub>)<sub>3</sub>]<sup>+</sup> (**B**) of 1.246 Å is significantly smaller than the C–C distances found in the above Mo complexes which range from 1.259 and 1.268 in the CO complexes to 1.267 and 1.280 Å in the other two. Conversely, the Ru–C distances are longer (2.320–2.322 Å) than the Mo–C distance (2.038–2.268 Å). Considering that the acetylenes in the Ru complex do not bear substituents so that steric effects are negligible, it can be concluded that the Ru–acetylene bonds are relatively weak. This is reflected by the high energy calculated for these complexes. On the other hand, the Ru–P bond (2.320 Å) is shorter than the corresponding bond in the initial bisacetonitrile complex **A**.

Among several conceivable pathways investigated, to be discussed later, the most favorable one involves formation of the metallacyclopentatriene **C** (Figure 7). The detailed structures of **B**, **C**, and the transition state **TS<sub>BC</sub>** are given in Figure 9. As the distances involving the acetylenes are the same, only one of them is given.

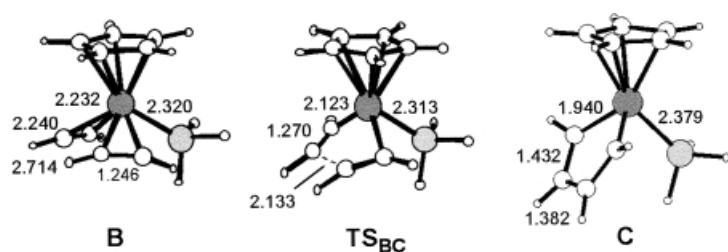


Figure 9. Relevant distances (Å) in the optimized B3LYP geometries of the bisacetylene complex **B**, the metallacyclopentatriene **C**, and the transition state **TS<sub>BC</sub>**.

As the reaction proceeds, the new C...C bond starts to form and the C...C distance decreases from 2.714 in **B** to 2.133 in **TS<sub>BC</sub>**, to reach 1.382 Å in species **C**, characteristic of a C=C bond. At the same time, the two acetylene groups must reorient themselves, so that two of the Ru–C bonds become stronger (distances decrease from 2.232 (**B**), via 2.123 (**TS<sub>BC</sub>**) to 1.940 (**C**)), and the other two weaker (2.240, 2.344, 2.901 Å, respectively). The C<sub>4</sub>Ru cycle is essentially planar and a strong alternation of bonds is observed. These changes occur smoothly, and the transition state occupies an intermediate position. It comes closer to the bisacetylene complex than to the metallacycle, since the C<sub>α</sub>–C<sub>β</sub> distances are still rather short, exhibiting triple-bond character (1.270 compared to

1.246 Å in the starting structure), while C<sub>β</sub>–C<sub>β'</sub> is still some distance away from a bonding distance (2.133 Å).

The formation of the metallacyclopentatriene is symmetry-allowed, according to an extended Hückel qualitative Walsh diagram (Supporting Information, Figure S1). The calculated activation barrier for this process is 8.5 kcal mol<sup>-1</sup>, the reaction being exothermic by 40.1 kcal mol<sup>-1</sup>. A comparable system has been studied by Albright and co-workers,<sup>[26]</sup> given by the formation of cobaltacyclopentadiene from [CpCo(C<sub>2</sub>H<sub>2</sub>)<sub>2</sub>]. In this case, the activation energy is slightly higher (12.8 kcal mol<sup>-1</sup>), although the process is less exothermic (13.1 kcal mol<sup>-1</sup>). The structural features of the two metallacycles are also significantly different, as in **C** the C<sub>α</sub>–C<sub>β</sub> distance (1.430 Å) is close to that of a single bond (1.34 Å for Co); C<sub>β</sub>–C<sub>β'</sub>, on the other hand, is very long for cobalt (1.49 Å) and much shorter (1.382 Å) in **C**. The metal–carbon bonds are comparable in both cases (1.92 Å for Co, 1.940 Å for Ru), but this bond length is very short for a Ru–C bond, suggesting a very strong bond. Despite the fact that a metallacyclopentatriene complex has been obtained in this work (**10**, in Scheme 2), it could not be structurally characterized owing to its short lifetime in solution. Therefore, the calculated structure **C** can only be compared to related species containing [CpRuBr] and [RuCp\*Br] fragments.<sup>[10a,g,h]</sup> The Ru–C and C<sub>β</sub>–C<sub>β'</sub> distances are the same (1.946 and 1.377 Å), while the C<sub>α</sub>–C<sub>β</sub> distance is slightly shorter but still very similar (1.403 Å). The agreement is very good considering the different coligands. To interpret the bonding in **C**, a schematic diagram was drawn, based on extended Hückel calculations<sup>[28]</sup> showing the interaction between the [CpRu(PH<sub>3</sub>)<sub>3</sub>]<sup>3+</sup> fragment and the C<sub>4</sub>H<sub>4</sub><sup>2-</sup> ligand (Figure 10).

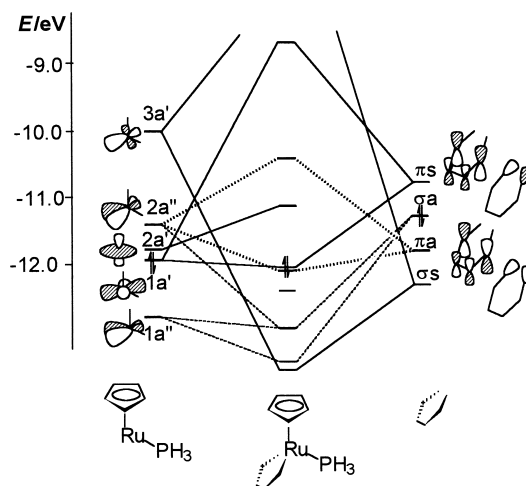


Figure 10. Schematic molecular orbital diagram showing the interaction between the [CpRu(PH<sub>3</sub>)<sub>3</sub>]<sup>3+</sup> (left) and [C<sub>4</sub>H<sub>4</sub>]<sup>2-</sup> (right) fragments.

The four orbitals of the butadienyl ligand that are relevant for binding to the metal fragment are depicted on the right side of Figure 10. The LUMO (π<sub>s</sub>) corresponds to the π<sub>3</sub> orbital of butadiene, while the HOMO (σ<sub>a</sub>) is the antisymmetric combination of the two carbon lone pairs; below come the π<sub>2</sub>-like orbital of butadiene (π<sub>a</sub>), followed by the symmetric combination of the two carbon lone pairs (σ<sub>s</sub>).



Three of these four orbitals are involved in strong interactions with acceptor fragment orbitals of  $[\text{CpRu}(\text{PH}_3)]^{3+}$ , the remaining interaction being a back-donation component from  $1a''$  to the LUMO. The two  $\sigma$  interactions involving  $\sigma_a$  and  $\sigma_s$  are the strongest, as expected, owing to better overlap between the fragment orbitals, while  $\pi$  donation is stronger than  $\pi$ -back donation. From this analysis, it is revealed that the two Ru–C bonds possess double-bond character, since on average each consists of  $\sigma + \pi$  bonds. Therefore, the  $\text{C}_4\text{Ru}$  cycle is indeed better described, as proposed above, as a metallacyclopentatriene rather than a metallacyclopentadiene, while the Co derivative has more metallacyclopentadiene character.<sup>[28]</sup> This bonding model thus sheds light on the origin of the strength of the Ru–C bonds and accounts for the high stability of the ruthenium metallacyclopentatriene **C** compared to that of its Co analogue. Interestingly, the reaction at the Ru center is much more exothermic and requires less activation energy than the Co system. The smaller activation energy is related to the structural similarity between the reagent **B** and the transition state **TS<sub>BC</sub>**. This species is known to undergo further reactions, with phosphine migration being the most frequent one, as long as a suitable phosphine is present.

The conversion of the metallacyclopentatriene **C** into the final allylcarbene complex **E** (Figure 7) proceeds with relatively small activation barriers, the rate-limiting step being an initial distortion to produce the intermediate **D**. Bending of the metallacycle takes place, and the  $\text{C}_\beta$ -carbon atoms approach the metal (these distances become 2.518 and 2.601 Å, already typical of weak bonds). Conversely, at the other side of the molecule, the Ru– $\text{C}_\alpha$  bond stretches and this carbon atom starts to form a new  $\text{C}_\alpha$ –P bond (2.450 Å). This feature is already evident in the transition state **TS<sub>CD</sub>** and the activation energy is 20.3 kcal mol<sup>−1</sup>. **TS<sub>CD</sub>** is much closer to **D** than **C**. The final transformation involves complete Ru–P bond breaking and formation of the  $\text{C}_\alpha$ –P bond, with simultaneous formation of the allyl carbene, and adjustments of the carbon chain, namely the formation of Ru– $\text{C}_\beta$  bonds. The Ru– $\text{C}_\beta$  distances in **E** are 2.198 and 2.267 Å and Ru– $\text{C}_\alpha$  2.146 and 1.911 Å. This last distance is much shorter than the three others and is assigned as a carbenic bond.

This new intermediate, **D**, makes the conversion of **C** into **E** easier, since the new Ru– $\text{C}_\beta$  bonds start to be formed before Ru–P bond breaking, requiring less energy. To understand this process, a detailed comparison between the species involved is needed. The most relevant parameters, Wiberg indices and NPA charges (italics), are given in Figure 11. In the case that the values are the same on both sides of each molecule, only one set is shown. The metallacyclopentatriene **C** shows two strong Ru–C bonds and one strong C–C bond,

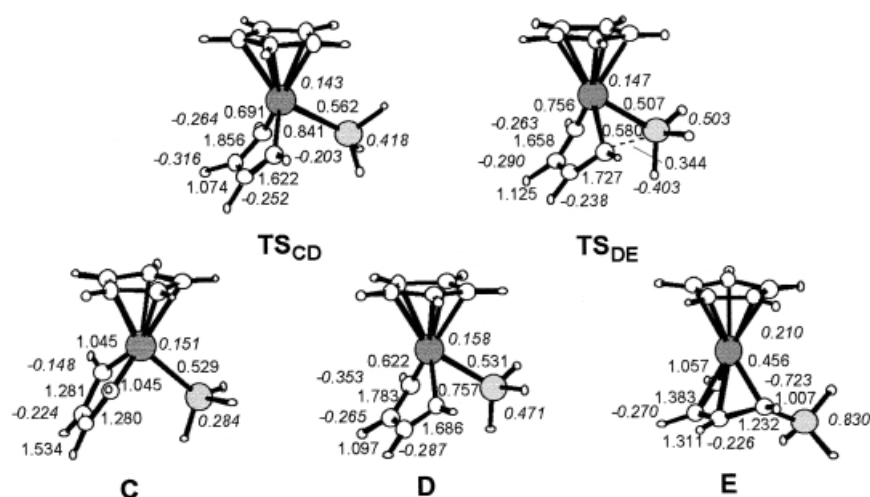


Figure 11. Wiberg indices and NPA charges (italics) in the optimized B3LYP geometries of the equilibrium structures **C**, **D**, **E**, and the transition states **TS<sub>CD</sub>** and **TS<sub>DE</sub>**.

with a Wiberg index typical of a double bond (Ru–C 1.045, C=C 1.534). The charges on P and the  $\alpha$ -carbon atoms are 0.248 and −0.145 (−0.148), respectively. On the other hand, the next intermediate **D** exhibits different bonding and is better described as a metallacycle. The Ru–C Wiberg indices have dropped to only 0.691 and 0.562, while two C=C bonds are present (1.783, 1.686) and the previously double bond became weaker (1.097). The P atom obtains an increasingly positive charge along the proposed pathway (from 0.284, to 0.471, to 0.830).

There is a problem with the pathway shown in Figure 7 in that the intermediate **C** is lower in energy than the final product **E**. This may arise from the use of the model phosphine  $\text{PH}_3$  instead of a more nucleophilic and also bulkier phosphine. The geometries of **C** and **E** containing both  $\text{PH}_3$  and  $\text{PMe}_3$  were optimized by using a smaller basis set, and single-point calculations were performed with the standard basis set. A similar procedure was used to compare the relative energies of **C** and **E** when the phosphine was replaced with  $\text{AsH}_3$  or  $\text{SbH}_3$ . The first immediate conclusion is that the reaction becomes thermodynamically favored for trimethylphosphine (−9.5 kcal mol<sup>−1</sup>) contrary to what happens with  $\text{PH}_3$  (5.9 kcal mol<sup>−1</sup>). On the other hand, we can compare the series of ligands where P is replaced by As and Sb, noticing that this reaction becomes progressively thermodynamically less favorable as one moves down the group ( $\text{AsH}_3$ , 6.5 kcal mol<sup>−1</sup>;  $\text{SbH}_3$ , 13.9 kcal mol<sup>−1</sup>). Arsines and stibines therefore have less tendency to migrate and their complexes may follow a different pathway.

An alternative pathway to afford allyl carbenes has also been considered in which intramolecular nucleophilic attack of  $\text{PH}_3$  at a coordinated  $\text{HC}\equiv\text{CH}$  ligand gives an intermediate  $\eta^2$ -vinyl complex. In the case of Mo and Re, it has been demonstrated that  $\eta^2$ -vinyl complexes are able to react with a further alkyne molecule to give allyl carbenes.<sup>[29]</sup> DFT calculations, however, revealed that a possible  $\eta^2$ -vinyl complex  $[\text{RuCp}(\eta^2\text{-CH=CH-PH}_3)(\eta^2\text{-HCCH})]^+$  (**K**) is found to lie as high as 17.8 kcal mol<sup>−1</sup> above the bisacetylene complex **B** (see Supporting Information, Figure S2). Although the transition state connecting **B** and **K** is missing, its energy is

expected to be much higher than that of the  $\eta^2$ -vinyl intermediate. It is therefore concluded that in the case of ruthenium, a pathway proceeding via an  $\eta^2$ -vinyl intermediate is very unlikely.

As mentioned above, the formation of cyclobutadiene complexes has been observed only in the reaction of **1a** with  $\text{PhC}\equiv\text{CPh}$ . In contrast, according to DFT calculations, the formation of a cyclobutadiene complex is thermodynamically favorable by  $-27 \text{ kcal mol}^{-1}$  (the optimized structure of the model cyclobutadiene complex  $[\text{RuCp}(\eta^4\text{-C}_4\text{H}_4)(\text{PH}_3)]^+$  (**F**) is shown in Figure 7). It is therefore concluded that cyclobutadiene complexes are not formed for kinetic reasons. In fact,  $[2+2]$  cycloadditions of acetylenes coordinated to the isoelectronic  $\text{CpCo}$  fragment are symmetry forbidden if  $C_s$  symmetry is preserved.<sup>[26]</sup> Since the same symmetry restrictions apply to the present  $[\text{RuCp}(\text{PH}_3)]^+$  system, both direct conversion of **B** to **F** by means of  $[2+2]$  cycloaddition and reductive cyclization, transforming **C** to **F**, are symmetry-forbidden processes. Accordingly, a large energy barrier can be expected. The complete mechanism for the formation of the  $\eta^4$ -cyclobutadiene complex (**F**) from the bis(acetylene) intermediate (**B**) will be the subject of a forthcoming paper.

### The monoacetylene precursor

**Formation of allenyl carbenes:** It has been found that under certain conditions only one molecule of acetylene binds to the Ru center with one of the acetonitrile ligands of **A** remaining. The coordination of only one acetylene molecule is independent of the concentration of acetylene and depends only on the nature of the substituents. It is rapidly followed by conversion to a vinylidene complex. Since this type of process has been widely studied from a theoretical point of view by several authors using several methods,<sup>[30]</sup> it will not be analyzed here. The presence of such an intermediate has

been proven by spectroscopic means. Therefore, we study here the subsequent reaction to allenyl carbenes as presented in Figure 12.

The substitution of acetonitrile by acetylene to afford the new vinylidene complex **I** is a slightly endothermic reaction in our model ( $3.5 \text{ kcal mol}^{-1}$ ), with an activation barrier of  $31.7 \text{ kcal mol}^{-1}$ , determined by the dissociation of the acetonitrile ligand. The fact that the acetylene complex has a higher energy than the acetonitrile derivative has been discussed before. After coordination of another molecule of acetylene, intermediate **I** is formed and easily converted into the final allenyl complex, **J**. The relevant structural data are shown in Figure 13.

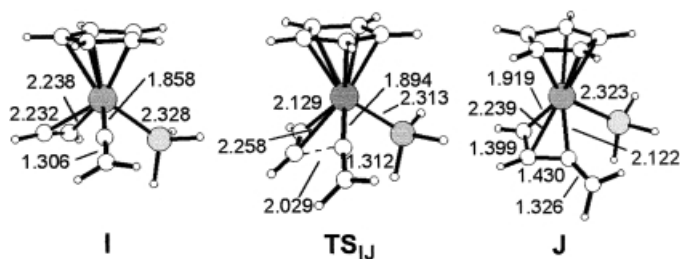


Figure 13. Relevant distances (Å) in the optimized B3LYP geometries of the acetylenevinylidene **I**, the allenyl carbene **J**, and the transition state **TS<sub>IJ</sub>**.

Notably, the Ru–P bond is barely affected by the reaction. On the other hand, as the  $C_\alpha$  atom of the vinylidene becomes involved in another bond to an acetylenic carbon atom, both the Ru– $C_\alpha$  and the  $C_\alpha$ – $C_\beta$  bonds become weaker, as can be seen in Figure 13. In the transition state **TS<sub>IJ</sub>** the new carbon bond has not yet formed ( $2.029 \text{ Å}$ ), although the two ligands have approached each other. In the final product **J**, the Ru–C bond that is significantly shorter than the others ( $1.919 \text{ Å}$ ) is assigned as a carbenic bond.

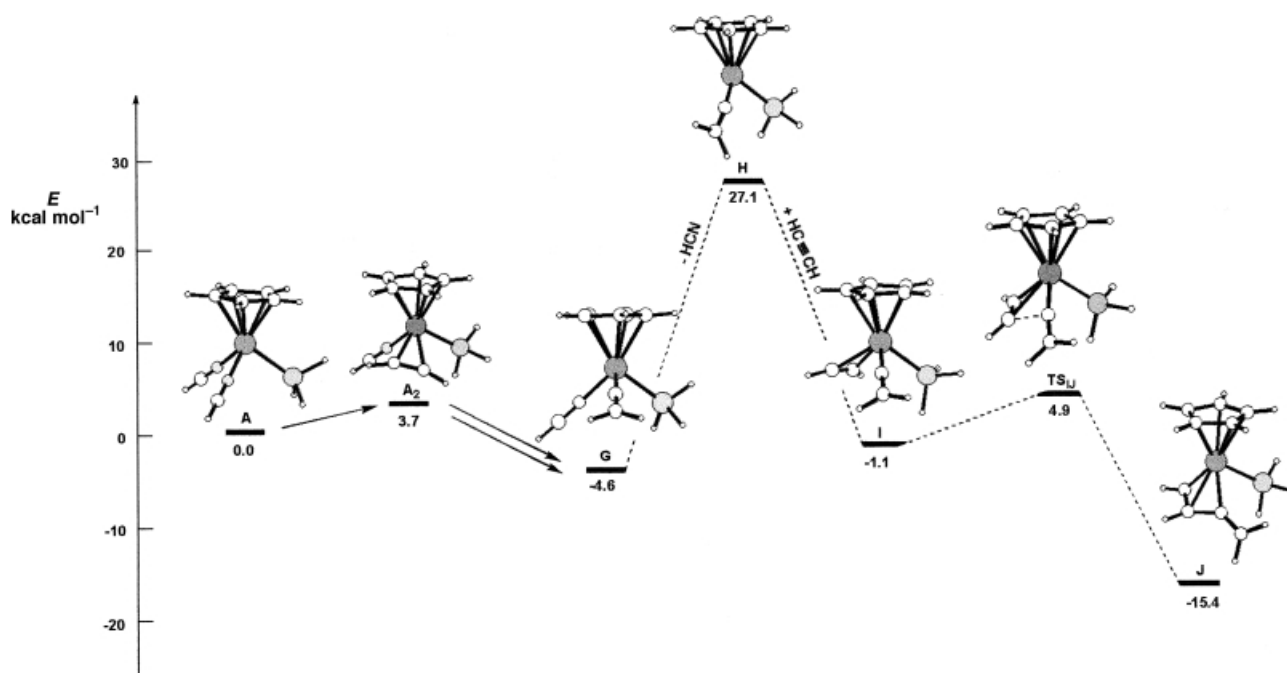


Figure 12. Profile of the B3LYP potential energy surfaces for the conversion of the bis-nitrile complex **A** into the allenyl carbene **J**.

## Conclusion

In summary, the reactions of alkynes with  $[\text{RuCp}(\text{PR}_3)_2(\text{CH}_3\text{CN})_2]\text{PF}_6$  ( $\text{R} = \text{Me, Ph, Cy}$ ) to give either allyl carbene or butadienyl carbene complexes have been elucidated. In both cases the first step is oxidative coupling of the alkyne to afford a cationic metallacyclopentatriene intermediate. The reactivity of the latter depends on the nucleophilicity of the phosphine as well as the presence of  $\alpha$ -alkyl substituents. Ligand migration leads to allyl carbenes, while a 1,2-hydrogen shift gives butadienyl carbenes. Therefore, owing to their strong electrophilic character, cationic metallacyclopentatriene complexes do not catalyze cyclotrimerizations. Cyclobutadiene formation is observed in only one case and seems to be an exception. An alternative reaction proceeds via vinylidene intermediates that are able to react with another alkyne moiety to give allenyl carbene complexes. This reaction is restricted to systems featuring bulky coligands such as  $\text{PPh}_3$  and  $\text{PCy}_3$  and strong electron-donating alkynes such as ethynylferrocene and ethynylruthenocene. DFT calculations support the experimental findings and identify metallacyclopentatriene and vinylidene complexes, respectively, as important intermediates in the formation of allyl and allenyl carbenes.

## Experimental Section

**General procedures:** All manipulations were performed under an inert atmosphere of argon by using Schlenk techniques. All chemicals were standard reagent grade and used without further purification. The solvents were purified according to standard procedures.<sup>[31]</sup> The deuterated solvents were purchased from Aldrich and dried over 4 Å molecular sieves.  $[\text{RuCp}(\text{PMe}_3)(\text{CH}_3\text{CN})_2]\text{PF}_6$  (**1a**),  $[\text{RuCp}(\text{PPh}_3)(\text{CH}_3\text{CN})_2]\text{PF}_6$  (**1b**),  $[\text{RuCp}(\text{PCy}_3)(\text{CH}_3\text{CN})_2]\text{PF}_6$  (**1c**), ethynylcobaltocenium hexafluorophosphate ( $[\text{HC}\equiv\text{CCc}]\text{PF}_6$ ), ethynylferrocene ( $\text{HC}\equiv\text{Cfc}$ ) and ethynylruthenocene ( $\text{HC}\equiv\text{Crc}$ ) were prepared according to the literature.<sup>[2, 32]</sup> The syntheses and characterization of complexes **2a–d**, **2g**, **2l**, **2n**, **2o**, **3f**, **3d**, **3g**, **4a**, **9a**, **9b**, **10**, and **11a–c** have been already reported previously.<sup>[4, 5]</sup>  $^1\text{H}$ ,  $^{13}\text{C}\{^1\text{H}\}$ , and  $^{31}\text{P}\{^1\text{H}\}$  NMR spectra were recorded on a Bruker AVANCE-250 spectrometer.

**$[\text{CpRu}(\text{C}(\text{SiMe}_3)(\eta^3\text{-CHC}(\text{SiMe}_3)\text{CHPMe}_3)]\text{PF}_6$  (**2e**):** A 5 mm NMR tube was charged with **1a** (35 mg, 0.075 mmol) and was capped with a septum. A solution of  $\text{HC}\equiv\text{CSiMe}_3$  (22  $\mu\text{L}$ , 0.150 mmol) in  $[\text{D}_6]\text{acetone}$  (0.5 mL) was added by syringe and the sample was transferred to an NMR probe. A  $^1\text{H}$  NMR spectrum was recorded after 1 h showing the formation of **2e** in about 90% yield. This compound could not be isolated in pure form.  $^1\text{H}$  NMR (250.13 MHz,  $[\text{D}_6]\text{acetone}$ , 20 °C, TMS):  $\delta = 5.47$  (s, 1H;  $\text{H}^2$ ), 5.36 (s, 5H; Cp), 5.03 (d,  $J_{\text{PH}} = 10.7$  Hz, 1H;  $\text{H}^4$ ), 1.32 (d,  $J_{\text{PH}} = 13.7$  Hz, 9H;  $\text{PMe}_3$ ), 0.33 (s, 9H;  $\text{SiMe}_3$ ) 0.24 ppm (s, 9H;  $\text{SiMe}_3$ );  $^{13}\text{C}\{^1\text{H}\}$  NMR (62.86 MHz,  $[\text{D}_6]\text{acetone}$ , –30 °C, TMS):  $\delta = 279.0$  (d,  $J_{\text{CP}} = 4.3$  Hz;  $\text{C}^1$ ), 97.1 (d,  $J_{\text{CP}} = 2.4$  Hz;  $\text{C}^3$ ), 84.6 (s, 5C; Cp), 75.5 (d,  $J_{\text{CP}} = 2.4$  Hz;  $\text{C}^2$ ), 36.9 (d,  $J_{\text{CP}} = 66.5$  Hz;  $\text{C}^4$ ), 10.8 (d,  $J_{\text{CP}} = 56.7$  Hz, 3C;  $\text{PMe}_3$ ), –0.04 (s, 3C;  $\text{SiMe}_3$ ), –1.4 ppm (s, 3C;  $\text{SiMe}_3$ );  $^{31}\text{P}\{^1\text{H}\}$  NMR (101.26 MHz,  $[\text{D}_6]\text{acetone}$ , –30 °C,  $\text{H}_3\text{PO}_4$  (85%)):  $\delta = 32.7$  ( $\text{PMe}_3$ ), –142.7 ppm ( $\text{PF}_6^-$ ).

**$[\text{CpRu}(\text{C}(\text{Ph-}p\text{-OMe})(\eta^3\text{-CHC}(\text{Ph-}p\text{-OMe})\text{CHPMe}_3)]\text{PF}_6$  (**2f**):** A solution of **1a** (100 mg, 0.215 mmol) and  $\text{HC}\equiv\text{CPh-}p\text{-OMe}$  (64  $\mu\text{L}$ , 0.495 mmol) in  $\text{CH}_2\text{Cl}_2$  (3 mL) was stirred for 2 h at 25 °C. The color of the solution changed from yellow to dark violet. After the volume of solution was reduced to about 0.5 mL, the product was precipitated with  $\text{Et}_2\text{O}$  (10 mL). The violet solid was collected on a glass frit, washed with  $\text{Et}_2\text{O}$ , and dried under vacuum. Yield: 135 mg (88%).  $^1\text{H}$  NMR (250.13 MHz,  $[\text{D}_6]\text{acetone}$ , 20 °C, TMS):  $\delta = 8.08$  (d,  $J_{\text{HH}} = 8.5$  Hz, 2H;  $(\text{CH}_3\text{O})\text{C}_6\text{H}_2$ ), 7.61 (d,  $J_{\text{HH}} = 8.9$  Hz, 2H;  $(\text{CH}_3\text{O})\text{C}_6\text{H}_2$ ), 7.05 (d,  $J_{\text{HH}} = 8.5$  Hz, 2H;  $(\text{CH}_3\text{O})\text{C}_6\text{H}_2$ ), 6.95 (d,  $J_{\text{HH}} = 8.9$  Hz, 2H;  $(\text{CH}_3\text{O})\text{C}_6\text{H}_2$ ), 5.78 (s, 1H;  $\text{H}^2$ ), 5.30 (d,  $J_{\text{PH}} =$

10.4 Hz, 1H;  $\text{H}^4$ ), 5.26 (s, 5H; Cp), 3.90 (s, 3H;  $\text{OCH}_3$ ), 3.84 (s, 3H;  $\text{OCH}_3$ ), 1.49 ppm (d,  $J_{\text{PH}} = 13.7$  Hz, 9H;  $\text{PMe}_3$ );  $^{13}\text{C}\{^1\text{H}\}$  NMR (62.86 MHz,  $[\text{D}_6]\text{acetone}$ , 20 °C, TMS):  $\delta = 245.4$  (d,  $J_{\text{CP}} = 5.8$  Hz;  $\text{C}^1$ ), 163.2 (1C;  $\text{Ph}^4$ ), 160.5 (1C;  $\text{Ph}^4$ ), 135.4 (1C;  $\text{Ph}^1$ ), 133.9 (2C;  $\text{Ph}^2$ ), 133.7 (1C;  $\text{Ph}^1$ ), 129.9 (2C;  $\text{Ph}^2$ ), 115.4 (2C;  $\text{Ph}^3$ ), 114.3 (2C;  $\text{Ph}^3$ ), 103.7 (d,  $J_{\text{CP}} = 3.8$  Hz;  $\text{C}^3$ ), 83.9 (5C; Cp), 80.5 (1C;  $\text{C}^2$ ), 55.6 (1C;  $\text{OCH}_3$ ), 55.2 (1C;  $\text{OCH}_3$ ), 31.0 (d,  $J_{\text{CP}} = 73.9$  Hz;  $\text{C}^4$ ), 12.1 ppm (d,  $J_{\text{CP}} = 57.6$  Hz, 3C;  $\text{PMe}_3$ );  $^{31}\text{P}\{^1\text{H}\}$  NMR (101.26 MHz,  $[\text{D}_6]\text{acetone}$ , 20 °C,  $\text{H}_3\text{PO}_4$  (85%)):  $\delta = 34.1$  ( $\text{PMe}_3$ ), –143.0 ppm ( $\text{PF}_6^-$ ,  $J_{\text{PF}} = 704.3$  Hz); elemental analysis calcd (%) for  $\text{C}_{31}\text{H}_{30}\text{F}_6\text{O}_2\text{P}_2\text{Ru}$  (711.6): C 52.33, H, 4.25; found: C 52.30, H 4.27.

**$[\text{CpRu}(\text{C}(\text{C}(\text{C}(\eta^3\text{-CHC}(\text{C}(\text{C}(\text{H}(\text{PMe}_3)](\text{PF}_6)_3$  (**2h**):** A solution of **1a** (70 mg, 0.149 mmol) and  $[\text{HC}\equiv\text{CCc}]\text{PF}_6$  (112 mg, 0.313 mmol) in acetone (3 mL) was stirred at room temperature for 3 h whereupon the color of the solution changed from yellow to dark green. After the solvent was removed, the solid residue was redissolved in  $\text{CH}_2\text{Cl}_2$  (0.5 mL) and the product was precipitated with  $\text{Et}_2\text{O}$  (10 mL). The dark green solid was collected on a glass frit, washed with  $\text{Et}_2\text{O}$ , and dried under vacuum. Yield: 108 mg (89%).  $^1\text{H}$  NMR (250.13 MHz,  $[\text{D}_6]\text{acetone}$ , 20 °C, TMS):  $\delta = 6.74$ –6.67 (m, 2H; Cc;  $\text{H}^2$ ), 6.55 (m, 1H; Cc), 6.37 (m, 1H; Cc), 6.27 (m, 1H; Cc), 6.18 (m, 1H; Cc), 6.10–6.04 (m, 6H; Cc,  $\text{Cp}^{\text{Co}}$ ), 5.99 (m, 2H; Cc), 5.96 (s, 5H;  $\text{Cp}^{\text{Co}}$ ), 5.84 (d,  $J_{\text{HP}} = 6.0$  Hz;  $\text{H}^4$ ), 5.62 (s, 5H;  $\text{Cp}^{\text{Ru}}$ ), 1.53 ppm (d,  $J_{\text{HP}} = 13.6$  Hz, 9H;  $\text{PMe}_3$ );  $^{13}\text{C}\{^1\text{H}\}$  NMR (62.86 MHz,  $[\text{D}_6]\text{acetone}$ , 20 °C, TMS):  $\delta = 235.9$  (d,  $J_{\text{CP}} = 6.9$  Hz, 1C;  $\text{C}^1$ ), 106.8 (d,  $J_{\text{CP}} = 5.4$  Hz, 1C;  $\text{C}^3$ ), 99.7 (1C; Cc), 92.6 (d,  $J_{\text{CP}} = 3.1$  Hz, 1C; Cc), 88.5 (1C; Cc), 88.4 (1C; Cc), 87.0 (5C;  $\text{Cp}^{\text{Ru}}$ ), 86.8 (5C;  $\text{Cp}^{\text{Co}}$ ), 86.5 (5C;  $\text{Cp}^{\text{Co}}$ ), 86.1 (1C; Cc), 85.5 (2C; Cc), 85.4 (1C;  $\text{C}^4$ ), 85.0 (1C; Cc), 82.9 (1C; Cc), 81.9 (1C; Cc), 34.6 (d,  $J_{\text{CP}} = 72.1$  Hz, 1C;  $\text{C}^4$ ), 11.2 ppm (d,  $J_{\text{CP}} = 57.5$  Hz; 3C,  $\text{PMe}_3$ );  $^{31}\text{P}\{^1\text{H}\}$  NMR (101.26 MHz,  $[\text{D}_6]\text{acetone}$ , 20 °C,  $\text{H}_3\text{PO}_4$  (85%)):  $\delta = 37.2$  ( $\text{PMe}_3$ ), –143.0 ppm ( $J_{\text{PF}} = 709.0$  Hz,  $\text{PF}_6^-$ ); elemental analysis calcd (%) for  $\text{C}_{32}\text{H}_{34}\text{Co}_2\text{F}_{18}\text{P}_4\text{Ru}$  (1103.4): C 34.83; H 3.11; found: C 34.89; H 3.15.

**$[\text{CpRu}(\text{C}(\text{Et})(\eta^3\text{-C}(\text{Et})\text{C}(\text{Et})\text{C}(\text{Et})\text{PMe}_3)]\text{PF}_6$  (**2i**):** A solution of **1a** (26 mg, 0.055 mmol) and  $\text{EtC}\equiv\text{CEt}$  (13  $\mu\text{L}$ , 0.116 mmol) in  $\text{CD}_3\text{NO}_2$  (0.4 mL) was transferred to a NMR tube and kept at room temperature for 20 days. The color of the solution changed slowly from yellow to red. The reaction was monitored by NMR spectroscopy. Yield: 90%.  $^1\text{H}$  NMR (250.13 MHz,  $\text{CD}_3\text{NO}_2$ , 20 °C, TMS):  $\delta = 5.24$  (s, 5H; Cp), 2.78–1.73 (m, 4H;  $\text{CH}_2$ ), 1.55 (t,  $J_{\text{HH}} = 7.0$  Hz, 3H;  $\text{CH}_3$ ), 1.40 (d,  $J_{\text{HP}} = 13.1$  Hz, 9H;  $\text{PMe}_3$ ), 1.31 (t,  $J_{\text{HH}} = 7.1$  Hz, 3H;  $\text{CH}_3$ ), 1.23 (t,  $J_{\text{HH}} = 7.4$  Hz, 3H;  $\text{CH}_3$ ), 1.21–0.88 (m, 4H;  $\text{CH}_2$ ), 0.85 ppm (t,  $J_{\text{HH}} = 7.6$  Hz, 3H;  $\text{CH}_3$ );  $^{13}\text{C}\{^1\text{H}\}$  NMR (62.86 MHz,  $\text{CD}_3\text{NO}_2$ , 20 °C, TMS):  $\delta = 267.6$  (d,  $J_{\text{CP}} = 5.8$  Hz;  $\text{C}^1$ ), 112.9 (s, 1C;  $\text{C}^2$ ), 99.8 (s, 1C;  $\text{C}^3$ ), 83.7 (s, 5C; Cp), 35.5 (s, 1C;  $\text{CH}_2$ ), 32.4 (d,  $J_{\text{CP}} = 10.6$  Hz, 1C;  $\text{CH}_2$ ), 28.8 (d,  $J_{\text{CP}} = 19.3$  Hz;  $\text{C}^4$ ), 24.8 (d,  $J_{\text{CP}} = 2.9$  Hz, 1C;  $\text{CH}_2$ ), 22.0 (s, 1C;  $\text{CH}_2$ ), 18.6 (s, 2C;  $\text{CH}_3$ ), 17.3 (s, 2C;  $\text{CH}_3$ ), 13.1 ppm (d,  $J_{\text{CP}} = 58.6$  Hz, 3C;  $\text{PMe}_3$ );  $^{31}\text{P}\{^1\text{H}\}$  NMR (101.26 MHz,  $\text{CD}_3\text{NO}_2$ , 20 °C,  $\text{H}_3\text{PO}_4$  (85%)):  $\delta = 32.8$  ( $\text{PMe}_3$ ), –143.6 ppm ( $J_{\text{PF}} = 706.4$  Hz,  $\text{PF}_6^-$ ).

**$[\text{CpRu}(\text{C}(\text{Ph})(\eta^3\text{-C}(\text{Me})\text{C}(\text{Me})\text{C}(\text{Ph})\text{PMe}_3)]\text{PF}_6$  (**2j**)/ **$[\text{CpRu}(\text{C}(\text{Ph})(\eta^3\text{-C}(\text{Me})\text{C}(\text{Ph})\text{C}(\text{Me})\text{PMe}_3)]\text{PF}_6$  (**2k**):** Compound **1a** (100 mg, 0.213 mmol) was dissolved in  $\text{CH}_3\text{NO}_2$  (3 mL) and  $\text{PhC}\equiv\text{CMe}$  (53  $\mu\text{L}$ , 0.426 mmol) was added. The reaction mixture was kept at 60 °C for 10 h, whereupon the color of the solution changed from yellow to dark blue. The solvent was removed under reduced pressure and the residue was collected on a glass frit, washed with  $\text{Et}_2\text{O}$  ( $3 \times 3$  mL), and dried under vacuum. The two products were obtained in a 10:7 ratio and could not be separated by recrystallization or column chromatography. **2j**:  $^1\text{H}$  NMR (250.13 MHz,  $\text{CD}_3\text{NO}_2$ , 20 °C, TMS):  $\delta = 8.27$ –8.06 (m, 2H; Ph), 7.63–7.40 (m, 8H; Ph), 5.33 (s, 5H; Cp), 2.48 (d,  $J_{\text{PH}} = 1.1$  Hz, 3H;  $\text{CH}_3$ ), 2.36 (d,  $J_{\text{PH}} = 1.1$  Hz, 3H;  $\text{CH}_3$ ), 1.03 ppm (d,  $J_{\text{PH}} = 12.6$  Hz, 9H;  $\text{PMe}_3$ ). **2k**:  $^1\text{H}$  NMR (250.13 MHz,  $\text{CD}_3\text{NO}_2$ , 20 °C, TMS):  $\delta = 8.27$ –8.06 (m, 2H; Ph), 7.90–7.67 (m, 8H; Ph), 5.43 (s, 5H; Cp), 1.99 (d,  $J_{\text{PH}} = 0.7$  Hz, 3H;  $\text{CH}_3$ ), 1.86 (d,  $J_{\text{PH}} = 15.0$  Hz, 3H;  $\text{CH}_3$ ), 1.39 ppm (d,  $J_{\text{PH}} = 12.9$  Hz, 9H;  $\text{PMe}_3$ ). It was not possible to assign the  $^{13}\text{C}\{^1\text{H}\}$  and  $^{31}\text{P}\{^1\text{H}\}$  NMR resonances of **2j** and **2k**.  $^{13}\text{C}\{^1\text{H}\}$  NMR (62.86 MHz,  $\text{CD}_3\text{NO}_2$ , 20 °C, TMS):  $\delta = 246.2$  (d,  $J_{\text{PC}} = 6.4$  Hz, 1C;  $\text{C}^1$ ), 246.1 (d,  $J_{\text{PC}} = 5.1$  Hz, 1C;  $\text{C}^1$ ), 141.8, 141.7, 141.3, 140.8, 139.2, 139.1, 135.4, 135.4, 132.8, 132.6, 132.4, 132.3, 132.2, 131.0, 130.9, 130.5, 129.5, 129.4, 129.2, 129.1, 129.0, 128.9, 128.4 (24C; Ph), 114.0 (1C;  $\text{C}^3$ ), 107.5 (1C;  $\text{C}^3$ ), 94.7 (1C;  $\text{C}^2$ ), 92.0 (1C;  $\text{C}^2$ ), 86.32 (s, 5C; Cp), 82.42 (s, 5C; Cp), 57.4 (d,  $J_{\text{CP}} = 63.4$  Hz;  $\text{C}^4$ ), 43.4 (d,  $J_{\text{CP}} = 67.4$  Hz;  $\text{C}^4$ ), 27.8 (d,  $J_{\text{CP}} = 11.4$  Hz, 1C;  $\text{CH}_3$ ), 24.2 (1C;  $\text{CH}_3$ ), 17.5 (1C;  $\text{CH}_3$ ), 17.3 (1C;  $\text{CH}_3$ ), 14.8 (d,  $J_{\text{PC}} = 59.8$  Hz, 3C;  $\text{PMe}_3$ ), 12.3 ppm (d,  $J_{\text{PC}} = 57.2$  Hz, 3C;  $\text{PMe}_3$ );  $^{31}\text{P}\{^1\text{H}\}$  NMR (101.26 MHz,  $\text{CD}_3\text{NO}_2$ , 20 °C,  $\text{H}_3\text{PO}_4$  (85%)):  $\delta = 36.7$  ( $\text{PMe}_3$ ), 34.0 ( $\text{PMe}_3$ ), –143.2 ppm ( $\text{PF}_6^-$ ,  $J_{\text{PF}} = 706.9$  Hz).**

**[CpRu(=CH- $\eta^3$ -C(CH<sub>2</sub>)<sub>4</sub>CCHPMe<sub>3</sub>)]PF<sub>6</sub> (2m):** A solution of **1a** (107 mg, 0.228 mmol) in acetone (5 mL) was treated with 1,7-octadiyne (31  $\mu$ L, 0.228 mmol) and stirred for 1 h, whereupon the color of the solution turned red. After the volume of the solution was reduced to about 1 mL, Et<sub>2</sub>O (20 mL) was slowly added and a red microcrystalline precipitate was formed. The supernatant liquid was decanted and the solid was washed twice with Et<sub>2</sub>O and dried under vacuum. Yield: 99 mg (88 %). <sup>1</sup>H NMR (250.13 MHz, [D<sub>6</sub>]acetone, 20 °C, TMS):  $\delta$  = 12.18 (s, 1 H; H<sup>1</sup>), 5.20 (s, 5 H; Cp), 5.09 (d,  $J_{\text{PH}}$  = 9.8 Hz, 1 H; H<sup>2</sup>), 2.98 (m, 2 H; CH<sub>2</sub>), 2.25 (m, 2 H; CH<sub>2</sub>), 1.73 (m, 2 H; CH<sub>2</sub>), 1.56 (m, 2 H; CH<sub>2</sub>), 1.35 ppm (d,  $J_{\text{PH}}$  = 13.7 Hz, 9 H; PMe<sub>3</sub>); <sup>13</sup>C{<sup>1</sup>H} NMR (62.86 MHz, [D<sub>6</sub>]acetone, 20 °C, TMS):  $\delta$  = 242.9 (d,  $J_{\text{CP}}$  = 6.5 Hz, 1C; C<sup>1</sup>), 106.9 (d,  $J_{\text{CP}}$  = 5.1 Hz, 1C; C<sup>3</sup>), 83.7 (s, 5C; Cp), 70.0 (d,  $J_{\text{CP}}$  = 3.6 Hz, 1C; C<sup>2</sup>), 36.0 (d,  $J_{\text{CP}}$  = 4.3 Hz, 1C; CH<sub>2</sub>), 35.2 (d,  $J_{\text{CP}}$  = 74.1 Hz, 1C; C<sup>4</sup>), 26.1 (s, 1C; CH), 23.1 (s, 1C; CH<sub>2</sub>), 22.4 (s, 1C; CH<sub>2</sub>), 10.6 ppm (d,  $J_{\text{CP}}$  = 59.6 Hz, 3C; PMe<sub>3</sub>); <sup>31</sup>P{<sup>1</sup>H} NMR (101.26 MHz, [D<sub>6</sub>]acetone, 20 °C, H<sub>3</sub>PO<sub>4</sub> (85 %)):  $\delta$  = 32.5 (PMe<sub>3</sub>), –142.7 ppm ( $J_{\text{PF}}$  = 711.7 Hz, PF<sub>6</sub>); elemental analysis calcd (%) for C<sub>16</sub>H<sub>24</sub>F<sub>6</sub>P<sub>2</sub>Ru (493.4): C 38.95, H 4.90; found: C 39.14; H 4.95.

**[CpRu(=CH- $\eta^3$ -CHCHCHPPh<sub>3</sub>)]PF<sub>6</sub> (3a):** This complex has been prepared in an analogous fashion to **2a** with **1b** and HC $\equiv$ CH as the starting materials. However, **3a** could not be isolated in pure form due to a subsequent rearrangement reaction. <sup>1</sup>H NMR (250.13 MHz, [D<sub>6</sub>]acetone, 20 °C, TMS):  $\delta$  = 11.36 (d,  $J$  = 3.1 Hz, 1 H; H<sup>1</sup>), 8.00–7.30 (m, 15 H; Ph), 7.02 (m, 1 H; H<sup>2</sup>), 6.21 (dd,  $J$  = 8.8 Hz,  $J$  = 7.2 Hz, 1 H; H<sup>4</sup>), 5.16 (s, 5 H; Cp), 5.07 ppm (t,  $J$  = 3.3 Hz, 1 H; H<sup>3</sup>); <sup>13</sup>C{<sup>1</sup>H} NMR (62.86 MHz, [D<sub>6</sub>]acetone, 20 °C, TMS):  $\delta$  = 247.1 (1C; C<sup>1</sup>), 136.0–128.0 (18C; PPh<sub>3</sub>), 92.7 (1C; C<sup>3</sup>), 88.1 (1C; C<sup>2</sup>), 86.4 (5C; Cp), 35.8 ppm (d,  $J_{\text{CP}}$  = 69.1 Hz; C<sup>4</sup>); <sup>31</sup>P{<sup>1</sup>H} NMR (101.26 MHz, [D<sub>6</sub>]acetone, 20 °C, H<sub>3</sub>PO<sub>4</sub> (85 %)):  $\delta$  = 33.2 (PPh<sub>3</sub>), –144.0 ppm (PF<sub>6</sub>).

**[CpRu(=C(Ph)- $\eta^3$ -CHC(Ph)CHPPh<sub>3</sub>)]PF<sub>6</sub> (3b):** This complex has been prepared in an analogous fashion to **2a** with **1b** (105 mg, 0.160 mmol) and HC $\equiv$ CPh (58  $\mu$ L, 0.320 mmol) as the starting materials. Yield: 113 mg (89 %). <sup>1</sup>H NMR (250.13 MHz, CD<sub>3</sub>NO<sub>2</sub>, 20 °C, TMS):  $\delta$  = 7.80–7.25 (m, 25 H; Ph), 6.09 (d,  $J_{\text{PH}}$  = 9.6 Hz, 1 H; H<sup>2</sup>), 5.62 (s, 1 H; H<sup>3</sup>), 5.19 ppm (s, 5 H; Cp); <sup>13</sup>C{<sup>1</sup>H} NMR (62.86 MHz, CD<sub>3</sub>NO<sub>2</sub>, 20 °C, TMS):  $\delta$  = 249.7 (d,  $J_{\text{CP}}$  = 6.6 Hz; C<sup>1</sup>), 143.2–122.1 (30C; Ph), 103.5 (d,  $J_{\text{CP}}$  = 4.0 Hz; C<sup>3</sup>), 86.9 (s, 5C; Cp), 78.2 (d,  $J_{\text{CP}}$  = 2.7 Hz; C<sup>2</sup>), 31.5 ppm (d,  $J_{\text{CP}}$  = 67.7 Hz; C<sup>4</sup>); <sup>31</sup>P{<sup>1</sup>H} NMR (101.26 MHz, CD<sub>3</sub>NO<sub>2</sub>, 20 °C, H<sub>3</sub>PO<sub>4</sub> (85 %)):  $\delta$  = 29.9 (PPh<sub>3</sub>), –143.5 ppm (PF<sub>6</sub>); elemental analysis calcd (%) for C<sub>39</sub>H<sub>47</sub>F<sub>6</sub>P<sub>2</sub>Ru (792.8): C 59.08, H 5.97; found: C 59.22, H 5.87.

**[CpRu(=C(C<sub>6</sub>H<sub>9</sub>)- $\eta^3$ -CHC(C<sub>6</sub>H<sub>9</sub>)CHPPh<sub>3</sub>)]PF<sub>6</sub> (3c):** A solution of **1b** (200 mg, 0.319 mmol) and 1-ethynylcyclohexene (83  $\mu$ L, 0.701 mmol) in CH<sub>3</sub>NO<sub>2</sub> (5 mL) was stirred at room temperature for 20 h. The color of the solution changed from yellow to dark brown. After removal of the solvent, the residue was redissolved in CH<sub>2</sub>Cl<sub>2</sub> (2 mL) and Et<sub>2</sub>O (ca. 10 mL) was added. A yellow precipitate was formed and the solution turned dark violet. The solid was removed by filtration and the filtrate was evaporated to dryness. The remaining dark red solid was collected on a glass frit, washed with petroleum ether, and dried under vacuum. Yield: 110 mg (45 %). <sup>1</sup>H NMR (250.13 MHz, CDCl<sub>3</sub>, 20 °C, TMS):  $\delta$  = 7.88–7.34 (m, 15 H; Ph), 6.33 (m, 1 H; C<sub>6</sub>H<sub>9</sub>), 5.71 (m, 1 H; C<sub>6</sub>H<sub>9</sub>), 5.56 (d,  $J_{\text{HP}}$  = 10.4 Hz, 1 H; H<sup>4</sup>), 5.02 (s, 5 H; Cp), 4.84 (s, 1 H; H<sup>2</sup>), 2.66–1.32 ppm (m, 16 H; C<sub>6</sub>H<sub>9</sub>); <sup>13</sup>C{<sup>1</sup>H} NMR (62.86 MHz, CDCl<sub>3</sub>, 20 °C, TMS):  $\delta$  = 251.2 (d,  $J_{\text{CP}}$  = 6.5 Hz; C<sup>1</sup>), 142.2 (1C; C=CH), 139.4 (1C; C=CH), 139.0 (d,  $J_{\text{CP}}$  = 4.4 Hz; C=CH), 134.5 (d,  $J_{\text{CP}}$  = 12.0 Hz, 6C; Ph<sup>2,6</sup>), 134.4 (s, 3C; Ph<sup>4</sup>), 129.6 (d,  $J_{\text{CP}}$  = 12.0 Hz, 6C; Ph<sup>3,5</sup>), 128.8 (1C; C=CH), 122.0 (d,  $J_{\text{CP}}$  = 87.2 Hz, 3C; Ph<sup>1</sup>), 104.7 (d,  $J_{\text{CP}}$  = 4.4 Hz, 1C; C<sup>3</sup>), 84.5 (5C; Cp), 75.2 (s, 1C; C<sup>2</sup>), 29.5, 27.4, 27.3 (6C; CH<sub>2</sub>), 26.5 (d,  $J_{\text{CP}}$  = 66.5 Hz, 1C; C<sup>4</sup>), 26.4, 22.8, 22.2, 21.2 ppm (10C; CH<sub>2</sub>); <sup>31</sup>P{<sup>1</sup>H} NMR (101.26 MHz, CDCl<sub>3</sub>, 20 °C, H<sub>3</sub>PO<sub>4</sub> (85 %)):  $\delta$  = 28.0 (PPh<sub>3</sub>), –143.5 ppm ( $J_{\text{PF}}$  = 712.9 Hz, PF<sub>6</sub><sup>–</sup>); elemental analysis calcd (%) for C<sub>39</sub>H<sub>40</sub>P<sub>2</sub>F<sub>6</sub>Ru: (785.8): C 59.62, H 5.13, found: C 59.58, H 5.09.

**Reaction of 1b and 1c with ethynylcobaltocenium hexafluorophosphate ([HC $\equiv$ CC]<sup>+</sup>PF<sub>6</sub><sup>–</sup>):** A solution of **1b** (29 mg, 0.047 mmol) and [HC $\equiv$ CC]<sup>+</sup>PF<sub>6</sub><sup>–</sup> (35 mg, 0.100 mmol) in CD<sub>3</sub>NO<sub>2</sub> (0.4 mL) was kept in an NMR tube at room temperature. <sup>1</sup>H NMR and <sup>31</sup>P{<sup>1</sup>H} NMR spectra were taken every 30 min. After 30 min, 50 % of the allyl carbene complex [CpRu(=C(Cc)- $\eta^3$ -CHC(Cc)CHPPh<sub>3</sub>)](PF<sub>6</sub>)<sub>3</sub> (**3e**) was formed. <sup>1</sup>H NMR (250.13 MHz, CD<sub>3</sub>NO<sub>2</sub>, 20 °C, TMS):  $\delta$  = 7.82–7.40 (m, 15 H; Ph), 6.43 (d,  $J_{\text{HP}}$  = 12.5 Hz, 1 H; H<sup>4</sup>), 6.20 (s, 1 H; H<sup>2</sup>), 5.81 (s, 5 H; Cp<sup>Co</sup>), 5.69 (s, 5 H; Cp<sup>Co</sup>), 5.38 ppm (s, 5 H; Cp<sup>Ru</sup>); <sup>31</sup>P{<sup>1</sup>H} NMR (101.26 MHz, CD<sub>3</sub>NO<sub>2</sub>, 20 °C, H<sub>3</sub>PO<sub>4</sub> (85 %)):  $\delta$  = 32.7 (PPh<sub>3</sub>), 143.2 ppm (PF<sub>6</sub>). After 24 h **3e** is completely converted

into a rearrangement product. This reaction will be discussed in a forthcoming paper.

**[CpRu(=C(Me)- $\eta^3$ -C(CH<sub>2</sub>)<sub>3</sub>CC(Me)PPh<sub>3</sub>)]PF<sub>6</sub> (3g):** This complex has been prepared in an analogous fashion to **2l** with **1b** (100 mg, 0.159 mmol) and 2,7-nonadiyne (29  $\mu$ L, 0.191 mmol) as the starting materials. Yield: 95 mg (85 %). <sup>1</sup>H NMR (250.13 MHz, CD<sub>2</sub>Cl<sub>2</sub>, 20 °C, TMS):  $\delta$  = 7.76–7.45 (m, 15 H; Ph), 4.70 (s, 5 H; Cp), 3.18–3.04 (m, 1 H; CH<sub>2</sub>), 2.71–2.52 (m, 2 H; CH<sub>2</sub>), 2.21–1.83 (m, 2 H; CH<sub>2</sub>), 2.13 (d,  $J_{\text{PH}}$  = 16.0 Hz; CH<sub>3</sub>), 1.62–1.54 (m, 1 H; CH<sub>2</sub>), 1.17 ppm (s, 3 H; CH<sub>3</sub>); <sup>13</sup>C{<sup>1</sup>H} NMR (62.86 MHz, CD<sub>2</sub>Cl<sub>2</sub>, 20 °C, TMS):  $\delta$  = 256.1 (d,  $J_{\text{CP}}$  = 7.2 Hz, 1C; C<sup>1</sup>), 134.3 (d,  $J_{\text{CP}}$  = 9.0 Hz, 6C; Ph<sup>3,5</sup>), 134.1 (3C,  $J_{\text{CP}}$  = 44.9 Hz; Ph<sup>1</sup>), 134.0 (d,  $J_{\text{CP}}$  = 3.6 Hz, 3C; Ph<sup>4</sup>), 129.9 (d,  $J_{\text{CP}}$  = 10.8 Hz, 6C; Ph<sup>2,6</sup>), 115.1 (1C; C<sup>3</sup>), 99.1 (1C; C<sup>2</sup>), 85.0 (s, 5C; Cp), 39.0 (d,  $J_{\text{CP}}$  = 61.0 Hz, 1C; C<sup>4</sup>), 33.7 (1C; CH<sub>2</sub>), 29.3 (s, 1C; CH<sub>3</sub>), 27.3 (s, 1C; CH<sub>2</sub>), 26.3 (d,  $J_{\text{CP}}$  = 10.8 Hz, 1C; CH<sub>3</sub>), 24.4 ppm (s, 1C; CH<sub>2</sub>); <sup>31</sup>P{<sup>1</sup>H} NMR (101.26 MHz, CD<sub>2</sub>Cl<sub>2</sub>, 20 °C, H<sub>3</sub>PO<sub>4</sub> (85 %)):  $\delta$  = 36.7 (PPh<sub>3</sub>), –143.7 ppm ( $J_{\text{PF}}$  = 710.2 Hz, PF<sub>6</sub>); elemental analysis calcd (%) for C<sub>32</sub>H<sub>32</sub>F<sub>6</sub>P<sub>2</sub>Ru (693.6): C 55.41, H 4.65; found: C 55.37, H 5.70.

**[CpRu(=C(Me)- $\eta^3$ -CC(CH<sub>2</sub>)<sub>3</sub>C(Me)PCy<sub>3</sub>)]PF<sub>6</sub> (4b):** This complex has been prepared in an analogous fashion to **2l** with **1c** (70 mg, 0.103 mmol) and 2,7-nonadiyne (20  $\mu$ L, 0.133 mmol) as the starting materials in a solvent of CH<sub>3</sub>NO<sub>2</sub> (3 mL). Yield: 60 mg (82 %). <sup>1</sup>H NMR (250.13 MHz, [D<sub>6</sub>]acetone, 20 °C, TMS):  $\delta$  = 5.14 (s, 5 H; Cp), 2.81–2.27 (m, 2 H; CH<sub>2</sub>), 2.47 (s, 3 H; CH<sub>3</sub>), 2.33 (d,  $J_{\text{HP}}$  = 12.0 Hz, 3 H; CH<sub>3</sub>), 2.18–1.02 ppm (m, 37 H; PCy<sub>3</sub>, CH<sub>2</sub>); <sup>13</sup>C{<sup>1</sup>H} NMR (62.86 MHz, [D<sub>6</sub>]acetone, 20 °C, TMS):  $\delta$  = 252.5 (d,  $J_{\text{CP}}$  = 3.5 Hz, 1C; C<sup>1</sup>), 116.8 (1C; C<sup>2</sup>), 98.9 (1C; C<sup>3</sup>), 85.5 (s, 5C; Cp), 39.4 (d,  $J_{\text{CP}}$  = 19.3 Hz, 3C; Cy<sup>1</sup>), 35.3 (d,  $J_{\text{CP}}$  = 71.0 Hz, 1C; C<sup>4</sup>), 32.3 (1C; CH<sub>2</sub>), 31.1 (s, 1C; CH<sub>3</sub>), 28.5 (d,  $J_{\text{CP}}$  = 6.4 Hz, 1C; CH<sub>3</sub>), 27.9 (s, 3C; Cy<sup>4</sup>), 26.9 (d,  $J_{\text{CP}}$  = 11.3 Hz, 6C; Cy<sup>2,2</sup>), 26.6 (s, 6C; Cy<sup>3,3</sup>), 26.1 (s, 1C; CH<sub>2</sub>), 23.9 ppm (s, 1C; CH<sub>3</sub>); <sup>31</sup>P{<sup>1</sup>H} NMR (101.26 MHz, [D<sub>6</sub>]acetone, 20 °C, H<sub>3</sub>PO<sub>4</sub> (85 %)):  $\delta$  = 40.5 (PCy<sub>3</sub>), –143.0 ppm ( $J_{\text{PF}}$  = 705.3, PF<sub>6</sub><sup>–</sup>); elemental analysis calcd (%) for C<sub>32</sub>H<sub>50</sub>F<sub>6</sub>P<sub>2</sub>Ru (711.8): C 54.00, H 7.08; found: C 54.06, H 7.11.

**[CpRu( $\eta^4$ -C<sub>4</sub>Ph<sub>4</sub>)(PMe<sub>3</sub>)]PF<sub>6</sub> (5):** A solution of **1a** (95 mg, 0.202 mmol) and PhC $\equiv$ CPh (83 mg, 0.465 mmol) in CH<sub>3</sub>NO<sub>2</sub> (3 mL) was kept at 80 °C for 24 h. The color of the solution changed from yellow to green and then finally to dark orange. After that time the solvent was removed under vacuum, the remaining residue was dissolved in CH<sub>2</sub>Cl<sub>2</sub> (0.5 mL) and the product was precipitated with Et<sub>2</sub>O (10 mL) as an orange solid which was collected on a glass frit, washed with Et<sub>2</sub>O, and dried under vacuum. Yield: 130 mg (87 %). <sup>1</sup>H NMR (250.13 MHz, CD<sub>3</sub>NO<sub>2</sub>, 20 °C, TMS):  $\delta$  = 7.72–7.22 (m, 20 H; Ph), 5.28 (d,  $J_{\text{HP}}$  = 1.5 Hz, 5 H; Cp), 1.30 ppm (d,  $J_{\text{HP}}$  = 12.5 Hz; PMe<sub>3</sub>); <sup>13</sup>C{<sup>1</sup>H} NMR (62.86 MHz, CD<sub>3</sub>NO<sub>2</sub>, 20 °C, TMS):  $\delta$  = 130.8 (4C; Ph<sup>1</sup>), 130.4 (8C; Ph<sup>2,6</sup>), 128.8 (4C; Ph<sup>4</sup>), 128.4 (8C; Ph<sup>3,5</sup>), 90.5 (5C; Cp), 84.5 (4C; C<sub>4</sub>Ph<sub>4</sub>), 18.0 ppm (d,  $J_{\text{PC}}$  = 34.3 Hz, 3C; PMe<sub>3</sub>); <sup>31</sup>P{<sup>1</sup>H} NMR (101.26 MHz, CD<sub>3</sub>NO<sub>2</sub>, 20 °C, H<sub>3</sub>PO<sub>4</sub> (85 %)):  $\delta$  = 1.4 (PMe<sub>3</sub>), –142.7 ppm ( $J_{\text{PF}}$  = 707.8 Hz); elemental analysis calcd (%) for C<sub>36</sub>H<sub>34</sub>F<sub>6</sub>P<sub>2</sub>Ru (743.68): C 58.14, H 4.61; found: C 58.09, H 4.58.

**[CpRu( $\eta^6$ -C<sub>6</sub>H<sub>6</sub>-C $\equiv$ C-Ph)]PF<sub>6</sub> (6) and [CpRu(PPh<sub>3</sub>)<sub>2</sub>(CH<sub>3</sub>CN)]PF<sub>6</sub> (7):** A solution of **1b** (60 mg, 0.096 mmol) and PhC $\equiv$ CPh (37 mg, 0.210 mmol) in CH<sub>3</sub>NO<sub>2</sub> (3 mL) was stirred at 80 °C for 20 h. The solvent was removed and the residue treated with Et<sub>2</sub>O. The precipitate was filtered, washed with Et<sub>2</sub>O, and dried under vacuum. The two known products could not be separated by crystallization or column chromatography. The NMR spectra of **6** and **7** were in agreement with those reported in the literature. The reaction of **1c** with diphenylacetylene led to several intractable complexes together with small amounts of **6**.

**[CpRu(=C=CHSiMe<sub>3</sub>)(CH<sub>3</sub>CN)(PPh<sub>3</sub>)]PF<sub>6</sub> (8a):** HC $\equiv$ CSiMe<sub>3</sub> (10.1  $\mu$ L, 0.143 mmol) was added to a solution of **1b** (32 mg, 0.051 mmol) in CD<sub>3</sub>NO<sub>2</sub> (0.3 mL). The reaction was monitored by <sup>1</sup>H and <sup>31</sup>P NMR spectroscopy and was quantitative within 4 h. <sup>1</sup>H NMR (250.13 MHz, CD<sub>3</sub>NO<sub>2</sub>, 20 °C, TMS):  $\delta$  = 7.72–7.23 (m, 15 H; Ph), 5.23 (s, 5 H; Cp), 3.93 (d,  $J_{\text{HP}}$  = 4.0 Hz, 1 H; =C=CHSiMe<sub>3</sub>), 1.99 (d,  $J_{\text{HP}}$  = 1.3 Hz, 3 H; CH<sub>3</sub>CN), 0.20 ppm (s, 9 H; SiMe<sub>3</sub>); <sup>13</sup>C{<sup>1</sup>H} NMR ( $\delta$ , CD<sub>3</sub>NO<sub>2</sub>, 20 °C, TMS):  $\delta$  = 321.3 (d,  $J_{\text{CP}}$  = 17.3 Hz, 1C; =C=CHSiMe<sub>3</sub>), 133.9 (d,  $J_{\text{CP}}$  = 10.6 Hz, 6C; Ph<sup>2,6</sup>), 133.4 (d,  $J_{\text{CP}}$  = 47.0 Hz, 3C; C<sup>1</sup>), 131.3 (s, 3C; C<sup>4</sup>), 130.2 (s, 1C; CH<sub>3</sub>CN), 128.9 (d,  $J_{\text{CP}}$  = 10.5 Hz, 6C; Ph<sup>3,5</sup>), 100.1 (d,  $J_{\text{CP}}$  = 2.2 Hz, 1C; =C=CHSiMe<sub>3</sub>), 90.0 (d,  $J_{\text{CP}}$  = 1.8 Hz, 5C; Cp), 2.5 (1C; CH<sub>3</sub>CN), 0.1 ppm (s, 3C; SiMe<sub>3</sub>); <sup>31</sup>P{<sup>1</sup>H} NMR (101.26 MHz, CD<sub>3</sub>NO<sub>2</sub>, 20 °C, H<sub>3</sub>PO<sub>4</sub> (85 %)):  $\delta$  = 53.7 (PPh<sub>3</sub>), –143.5 ppm ( $J_{\text{PF}}$  = 707.1 Hz, PF<sub>6</sub><sup>–</sup>).

**[CpRu(=C=CH(SiMe<sub>3</sub>))(CH<sub>3</sub>CN)(PCy<sub>3</sub>)]PF<sub>6</sub> (8b):** HC $\equiv$ CSiMe<sub>3</sub> (14  $\mu$ L, 0.187 mmol) was added to a solution of **1c** (42 mg, 0.062 mmol) in CD<sub>3</sub>NO<sub>2</sub>

(0.3 mL). The reaction was monitored by  $^1\text{H}$  and  $^{31}\text{P}$  NMR spectroscopy. Compound **1c** was quantitatively converted into **8b** within 8 h.  $^1\text{H}$  NMR (250.13 MHz,  $\text{CD}_3\text{NO}_2$ , 20 °C, TMS):  $\delta$  = 5.40 (s, 5H; Cp), 4.06 (d,  $^4J_{\text{H,P}}$  = 2.5 Hz, 1H; =C=CH), 2.42 (d,  $J_{\text{H,P}}$  = 0.8 Hz, 3H;  $\text{CH}_3\text{CN}$ ), 2.25–1.14 (m, 33H;  $\text{PCy}_3$ ), 0.20 ppm (s, 9H;  $\text{SiMe}_3$ );  $^{13}\text{C}\{^1\text{H}\}$  NMR (62.86 MHz,  $\text{CD}_3\text{NO}_2$ , 20 °C, TMS):  $\delta$  = 320.5 (d,  $^2J_{\text{C,P}}$  = 15.4 Hz, 1C; =C=CH), 131.9 (s, 1C; CN), 100.2 (s, 1C; =C=CH), 88.8 (s, 5C; Cp), 37.8 (d,  $^4J_{\text{C,P}}$  = 23.0 Hz, 3C;  $\text{Cy}^1$ ), 30.2 (3C;  $\text{Cy}^4$ ), 27.8 (d,  $^2J_{\text{C,P}}$  = 9.6 Hz, 6C;  $\text{Cy}^{2,6}$ ), 26.3 (bs, 6C;  $\text{Cy}^{3,5}$ ), 2.92 (s, 1C;  $\text{CH}_3\text{CN}$ ), 0.98 ppm (s, 3C;  $\text{SiMe}_3$ );  $^{31}\text{P}\{^1\text{H}\}$  NMR (101.26 MHz,  $\text{CD}_3\text{NO}_2$ , 20 °C,  $\text{H}_3\text{PO}_4$  (85 %)):  $\delta$  = 59.0 ( $\text{PCy}_3$ ), –143.5 ppm ( $J_{\text{PF}} = 707.1$  Hz,  $\text{PF}_6^-$ ).

**[CpRu(=C(Rc- $\eta^2$ -CH=C=CH(Rc))PPh<sub>3</sub>)]PF<sub>6</sub> (**9c**):** This compound was prepared in an analogous fashion to **9a** with **1b** (200 mg, 0.319 mmol) and ethynylruthenocene (179 mg, 0.701 mmol). Yield: 270 mg (78 %).  $^1\text{H}$  NMR (250.13 MHz,  $\text{CD}_3\text{NO}_2$ , 20 °C, TMS):  $\delta$  = 7.96–7.05 (m, 15H; Ph), 5.83 (d,  $^5J_{\text{H,H}}$  = 3.0 Hz, 1H;  $\text{H}^2$ ), 5.80 (m, 1H; Rc), 5.53 (m, 1H; Rc), 5.34 (m, 1H; Rc), 5.31 (s, 5H;  $\text{Cp}^{\text{Ru}}$ ), 4.86 (s, 5H;  $\text{Cp}^{\text{Ru}}$ ), 4.80 (m, 1H; Rc), 4.60 (m, 2H; Rc), 4.43 (m, 1H; Rc), 4.24 (m, 1H; Rc), 4.21 (s, 5H;  $\text{Cp}^{\text{Ru}}$ ), 3.22 ppm (d,  $^5J_{\text{H,H}}$  = 3.0 Hz, 1H;  $\text{H}^4$ );  $^{13}\text{C}\{^1\text{H}\}$  NMR (62.86 MHz,  $\text{CD}_3\text{NO}_2$ , 20 °C, TMS):  $\delta$  = 272.1 (d,  $^2J_{\text{C,P}}$  = 9.0 Hz; C<sup>1</sup>), 132.8–128.6 (PPh<sub>3</sub>), 122.3 (d,  $^5J_{\text{C,P}}$  = 4.0 Hz; C<sup>4</sup>), 90.7 (5C;  $\text{Cp}^{\text{Ru}}$ ), 90.5 (d,  $^4J_{\text{C,P}}$  = 3.0 Hz; Rc), 84.3 (Rc), 82.3 (Rc), 80.4 (Rc), 77.9 (Rc), 77.8 (Rc), 76.6 (5C;  $\text{Cp}^{\text{Ru}}$ ), 71.7 (5C;  $\text{Cp}^{\text{Ru}}$ ), 71.6 (Rc), 71.3 (1C, C<sup>3</sup>), 71.1 (Rc), 69.7 (Rc), 30.7 ppm (d,  $^2J_{\text{C,P}}$  = 3.0 Hz; C<sup>2</sup>);  $^{31}\text{P}\{^1\text{H}\}$  NMR (101.26 MHz,  $\text{CD}_3\text{NO}_2$ , 20 °C,  $\text{H}_3\text{PO}_4$  (85 %)):  $\delta$  = 41.9 (PPh<sub>3</sub>), –146.9 ppm ( $\text{PF}_6^-$ ,  $J_{\text{PF}} = 707$  Hz); elemental analysis calcd (%) for  $\text{C}_{47}\text{H}_{40}\text{F}_6\text{P}_2\text{Ru}_3$  (1084.0): C 52.08, H 3.72; found: C 52.11, H 3.79.

**Crystal structure determinations:** Crystals of **2b**, **2g**, **3g** ·  $\frac{1}{2}\text{CH}_2\text{Cl}_2$ , **4b**, **5**, and **9c** ·  $\text{CH}_2\text{Cl}_2$  were obtained by gas diffusion of  $\text{Et}_2\text{O}$  into  $\text{CH}_2\text{Cl}_2$  solutions. Crystal data and experimental details are given in Table 3. All X-ray data were collected on a Bruker Smart CCD area detector diffractometer (graphite-monochromated  $\text{MoK}\alpha$  radiation,  $\lambda = 0.71073$  Å,  $0.3^\circ$   $\omega$ -scan frames covering complete spheres of the reciprocal space. Corrections for Lorentz and polarization effects, for crystal decay, and for absorption were applied (multi-scan method with the program SA-

DABS<sup>[33]</sup>). All structures were solved by direct methods using the program SHELXS97<sup>[34]</sup>. Structure refinements on  $F^2$  were carried out with program SHELXL97<sup>[35]</sup>. All non-hydrogen atoms were refined anisotropically. Most hydrogen atoms were inserted in idealized positions and were refined riding with the atoms to which they were bonded. Critical hydrogen atoms were refined in positional parameters without such restraints.

CCDC-176091 (**2b**), CCDC-176092 (**2g**), CCDC-176093 (**3g** ·  $\frac{1}{2}\text{CH}_2\text{Cl}_2$ ), CCDC-176094 (**4a**), CCDC-176095 (**5**), and CCDC-176097 (**9c** ·  $\text{CH}_2\text{Cl}_2$ ) contain the supplementary crystallographic data for this paper. These data can be obtained free of charge at [www.ccdc.cam.ac.uk/conts/retrieving.html](http://www.ccdc.cam.ac.uk/conts/retrieving.html) (or from the Cambridge Crystallographic Data Centre, 12 Union Road, Cambridge CB2 1EZ, UK (Fax: (+44) 1223-336-033; or e-mail: [deposit@ccdc.cam.ac.uk](mailto:deposit@ccdc.cam.ac.uk)).

**Computational techniques:** All calculations were performed by using the Gaussian98 software package<sup>[24]</sup> on the Silicon Graphics Cray Origin 2000 of the Vienna University of Technology, at IST and ITQB. The geometry and energy of the model complexes and the transition states were optimized at the B3LYP level<sup>[23]</sup> with the Stuttgart/Dresden ECP (sdd) basis set<sup>[36]</sup> to describe the electrons of the ruthenium atom. For all other atoms the 6–31g\*\* basis set was employed.<sup>[37]</sup> Frequency calculations were performed to confirm the nature of the stationary points, yielding one imaginary frequency for the transition states and none for the minima. Each transition state was further confirmed by following its vibrational mode downhill on both sides, and obtaining the minima presented on the reaction-energy profile. All geometries were optimized without constraints ( $C_1$  symmetry) and the energies were zero point corrected. A natural population analysis (NPA)<sup>[38]</sup> and the resulting Wiberg indices<sup>[39]</sup> were used for a detailed study of the electronic structure and bonding of the optimized species.

## Acknowledgements

Financial support by the “Fonds zur Förderung der wissenschaftlichen Forschung” is gratefully acknowledged (Project No. P14681-CHE).

Table 3. Details of the crystal structure determinations for the complexes **2b**, **2g**, **3g** ·  $\frac{1}{2}\text{CH}_2\text{Cl}_2$ , **4b**, **5**, and **9c** ·  $\text{CH}_2\text{Cl}_2$ .

|  | <b>2b</b>  | <b>2g</b>  | <b>3g</b> · $\frac{1}{2}\text{CH}_2\text{Cl}_2$                      | <b>4b</b>  | <b>5</b>   | <b>9c</b> · $\text{CH}_2\text{Cl}_2$                                   |
|--|--|--|--|--|--|--|
| formula  | $\text{C}_{24}\text{H}_{26}\text{F}_6\text{P}_2\text{Ru}$            | $\text{C}_{32}\text{H}_{34}\text{F}_6\text{FeP}_2\text{Ru}$        | $\text{C}_{32.5}\text{H}_{33}\text{ClF}_6\text{P}_2\text{Ru}$        | $\text{C}_{32}\text{H}_{30}\text{F}_6\text{P}_2\text{Ru}$            | $\text{C}_{36}\text{H}_{34}\text{F}_6\text{P}_2\text{Ru}$            | $\text{C}_{48}\text{H}_{42}\text{Cl}_2\text{F}_6\text{P}_2\text{Ru}_3$ |
| fw   | 591.46   | 807.30   | 736.05   | 711.73   | 743.64   | 1168.87  |
| cryst.size [mm]                                  | $0.60 \times 0.26 \times 0.06$                                       | $0.60 \times 0.06 \times 0.02$                                     | $0.50 \times 0.32 \times 0.04$                                       | $0.55 \times 0.32 \times 0.30$                                       | $0.50 \times 0.30 \times 0.20$                                       | $0.78 \times 0.39 \times 0.07$   |
| space group                                      | $P2_1$ (no. 4)   | $P2_1/n$ (no. 14)  | $Pbca$ (no. 61)  | $P2_1/n$ (no. 14)  | $P\bar{1}$ (no. 2)   | $P2_1/n$ (no. 14)  |
| <i>a</i> [Å]                                     | 11.154(2)  | 7.844(3)   | 19.112(9)  | 13.400(5)  | 11.013(8)  | 12.273(4)  |
| <i>b</i> [Å]                                     | 8.109(2)   | 21.281(9)  | 17.414(9)  | 17.623(7)  | 11.229(8)  | 14.515(5)  |
| <i>c</i> [Å]                                     | 13.897(2)  | 19.296(8)  | 38.391(19)   | 14.595(5)  | 15.813(12)   | 25.003(8)  |
| $\alpha$ [°]                                     |  |  |  |  | 99.89(2)   |  |
| $\beta$ [°]                                      | 97.76(1)   | 99.54(1)   |  | 103.01(1)  | 99.85(2)   | 94.19(2)   |
| $\gamma$ [°]                                     |  |  |  |  | 118.86(2)  |  |
| <i>V</i> [Å <sup>3</sup> ]                       | 1245.4(4)  | 3176(2)  | 12777(11)  | 3358(2)  | 1612(2)  | 4442(3)  |
| <i>Z</i>   | 2  | 4  | 16   | 4  | 2  | 4  |
| $\rho_{\text{calcd}}$ [g cm <sup>−3</sup> ]      | 1.577  | 1.688  | 1.531  | 1.408  | 1.532  | 1.748  |
| <i>T</i> [K]                                     | 296(2)   | 297(2)   | 297(2)   | 297(2)   | 297(2)   | 223(2)   |
| $\mu$ [mm <sup>−1</sup> ]( $\text{MoK}\alpha$ )  | 0.813  | 1.529  | 0.731  | 0.616  | 0.646  | 1.259  |
| <i>F</i> (000)                                   | 596  | 1624   | 5968   | 1480   | 756  | 2320   |
| absorption corr.                                 | multiscan  | multiscan  | multiscan  | multiscan  | multiscan  | multiscan  |
| transmiss. fact. min/max                         | 0.84/0.93  | 0.82/0.96  | 0.79/0.89  | 0.80/0.86  | 0.76/0.92  | 0.40/0.80  |
| $\theta_{\text{max}}$ [°]                        | 30   | 25   | 25   | 30   | 25   | 27   |
| index ranges                                     | $-15 \leq h \leq 15$<br>$-11 \leq k \leq 11$<br>$-19 \leq l \leq 19$ | $-9 \leq h \leq 9$<br>$-25 \leq k \leq 25$<br>$-22 \leq l \leq 22$ | $-22 \leq h \leq 22$<br>$-20 \leq k \leq 20$<br>$-43 \leq l \leq 45$ | $-18 \leq h \leq 18$<br>$-24 \leq k \leq 24$<br>$-20 \leq l \leq 20$ | $-13 \leq h \leq 12$<br>$-13 \leq k \leq 13$<br>$-18 \leq l \leq 18$ | $-15 \leq h \leq 15$<br>$-18 \leq k \leq 18$<br>$-31 \leq l \leq 31$   |
| no. of rflns measd                               | 18087  | 24175  | 113354   | 55149  | 16265  | 52617  |
| no. of unique rflns                              | 7191   | 5567   | 11038  | 9698   | 5629   | 9638   |
| no. of rflns $I > 2\sigma(I)$                    | 6573   | 3259   | 7144   | 7354   | 4285   | 8178   |
| no. of params                                    | 307  | 370  | 773  | 389  | 406  | 604  |
| $R_1$ ( $I > 2\sigma(I)$ ) <sup>[a]</sup>        | 0.026  | 0.051  | 0.047  | 0.041  | 0.053  | 0.034  |
| $R_1$ (all data)                                 | 0.031  | 0.106  | 0.087  | 0.057  | 0.068  | 0.044  |
| $wR_2$ (all data)                                | 0.066  | 0.141  | 0.133  | 0.124  | 0.148  | 0.085  |
| diff. Fourier peaks min/max [e Å <sup>−3</sup> ] | −0.41/0.41   | −0.49/0.68   | −0.44/0.65   | −0.49/0.60   | −1.06/1.04   | −0.70/0.79   |

[a]  $R_1 = \Sigma||F_o| - |F_c||/\Sigma|F_o|$ ,  $wR_2 = [\Sigma(w(F_o^2 - F_c^2)^2)/\Sigma(w(F_o^2)^2)]^{1/2}$ .

- [1] Y. Yamamoto, H. Kitahara, R. Ogawa, H. Kawaguchi, K. Tatsumi, K. Itoh, *J. Am. Chem. Soc.* **2000**, *122*, 4310, and references therein.
- [2] E. Rüba, W. Simanko, K. Mauthner, K. M. Soldouzi, C. Slugovc, K. Mereiter, R. Schmid, K. Kirchner, *Organometallics* **1999**, *18*, 3843.
- [3] C. Slugovc, E. Rüba, R. Schmid, K. Kirchner, *Organometallics* **1999**, *18*, 4230.
- [4] E. Becker, C. Slugovc, E. Rüba, C. Standfest-Hauser, K. Mereiter, R. Schmid, K. Kirchner, *J. Organomet. Chem.* **2002**, *649*, 55.
- [5] K. Mauthner, K. M. Soldouzi, K. Mereiter, R. Schmid, K. Kirchner, *Organometallics* **1999**, *18*, 4681.
- [6] E. Rüba, K. Mereiter, R. Schmid, K. Kirchner, *Chem. Commun.* **2001**, 1996.
- [7] E. Rüba, K. Mereiter, R. Schmid, K. Kirchner, H. Schottenberger, *J. Organomet. Chem.* **2001**, *637–639*, 70.
- [8] C. S. Yi, J. R. Torres-Lubian, N. Liu, A. L. Rheingold, I. A. Guzei, *Organometallics* **1998**, *17*, 1257, and references therein.
- [9] J. La Pahi, S. Derien, P. H. Dixneuf, *Chem. Commun.* **1999**, 1437.
- [10] For metallacyclopentatriene complexes see: a) M. O. Albers, P. J. A. de Waal, D. C. Liles, D. J. Robinson, E. Singleton, M. B. Wiege, *J. Chem. Soc. Chem. Commun.* **1986**, 1680; b) C. Gemel, A. La Pensée, K. Mauthner, K. Mereiter, R. Schmid, K. Kirchner, *Monatsh. Chem.* **1997**, *128*, 1189; c) L. Pu, T. Hasegawa, S. Parkin, H. Taube, *J. Am. Chem. Soc.* **1992**, *114*, 2712; d) W. Hirpo, M. D. Curtis, *J. Am. Chem. Soc.* **1988**, *110*, 5218; e) J. L. Kerschner, P. E. Fanwick, I. P. Rothwell, *J. Am. Chem. Soc.* **1988**, *110*, 8235; f) B. Hessen, A. Meetsma, F. van Bolhuis, J. H. Teuben, G. Helgesson, S. Jagner, *Organometallics* **1990**, *9*, 1925; g) C. Ernst, O. Walter, E. Dinjus, S. Arzberger, H. Görls, *J. Prakt. Chem.* **1999**, *341*, 801; h) Y. Yamada, J. Mizutani, M. Kurihara, H. Nishihara, *J. Organomet. Chem.* **2001**, *637–639*, 80.
- [11] R. G. Parr, W. Yang, *Density Functional Theory of Atoms and Molecules*, Oxford University Press, New York, **1989**.
- [12] Y. Wakatsuki, O. Nomura, K. Kitaura, K. Morokuma, H. Yamazaki, *J. Am. Chem. Soc.* **1983**, *105*, 1907.
- [13] For related  $\eta^3$ -allyl carbene complexes see: a) M. Crocker, M. Green, A. G. Orpen, H. P. Neumann, C. J. Schaverin, *J. Chem. Soc. Chem. Commun.* **1984**, 1351; b) L. Carlton, J. L. Davidson, P. Ewing, L. Manojlovic-Muir, K. W. Muir, *J. Chem. Soc. Chem. Commun.* **1985**, 1474; c) J. R. Morrow, T. L. Tonker, J. Templeton, *J. Am. Chem. Soc.* **1985**, *107*, 5004; d) M. Crocker, S. F. T. Froom, M. Green, K. R. Nagle, A. G. Orpen, D. M. Thomas, *J. Chem. Soc. Dalton Trans.* **1987**, 2803; e) M. Crocker, M. Green, K. R. Nagle, A. G. Orpen, H. P. Neumann, C. E. Morton, C. J. Schaverin, *Organometallics* **1990**, *9*, 1422; f) C. Ernst, O. Walter, E. Dinjus, *J. Organomet. Chem.* **2001**, *627*, 249.
- [14] M. Crocker, S. F. T. Froom, M. Green, K. R. Nagle, A. G. Orpen, D. M. Thomas, *J. Chem. Soc. Dalton Trans.* **1987**, 2803.
- [15] E. Rüba, K. Mereiter, K. M. Soldouzi, C. Gemel, R. Schmid, K. Kirchner, E. Bustelo, M. C. Puerta, P. Valerga, *Organometallics* **2000**, *19*, 5384.
- [16] B. Chaudret, X. He, Y. Huang, *J. Chem. Soc. Chem. Commun.* **1989**, 1844.
- [17] F. G. A. Stone, T. Blackmore, M. I. Bruce, *J. Chem. Soc. A*, **1971**, 2376.
- [18] E. Becker, E. Rüba, K. Mereiter, R. Schmid, K. Kirchner, *Organometallics* **2001**, *20*, 3851.
- [19] L. Pu, T. Hasegawa, S. Parkin, H. Taube, *J. Am. Chem. Soc.* **1992**, *114*, 7609.
- [20] a) C. Slugovc, K. Mereiter, R. Schmid, K. Kirchner, *Organometallics* **1998**, *17*, 827; b) D. M. Heinekey, C. E. Radzewich, *Organometallics* **1998**, *17*, 51; c) T. Bodnar, A. R. Cutler, *J. Organomet. Chem.* **1981**, *213*, C13; d) E. O. Fischer, W. Held, *J. Organomet. Chem.* **1976**, *112*, C59.
- [21] E. Rüba, E. K. Mereiter, R. Schmid, K. Kirchner, E. Bustelo, M. C. Puerta, P. Valerga, *Organometallics* **2002**, in press.
- [22] The structure of **9b** has also been determined by X-ray crystallography but is of poor quality. Nevertheless, structural data of **9b** have been deposited at the Cambridge Crystallographic Data Centre (CCDC-176096).
- [23] a) M. I. Bruce, *Chem. Rev.* **1991**, *91*, 197; b) M. C. Puerta, P. Valerga, *Coord. Chem. Rev.* **1999**, *193*, 977.
- [24] a) A. D. Becke, *J. Chem. Phys.* **1993**, *98*, 5648; b) B. Miehlich, A. Savin, H. Stoll, H. Preuss, *Chem. Phys. Lett.* **1989**, *157*, 200; c) C. Lee, W. Yang, G. Parr, *Phys. Rev. B* **1988**, *37*, 785.
- [25] M. J. Frisch, G. W. Trucks, H. B. Schlegel, G. E. Scuseria, M. A. Robb, J. R. Cheeseman, V. G. Zakrzewski, J. A. Montgomery, Jr., R. E. Stratmann, J. C. Burant, S. Dapprich, J. M. Millam, A. D. Daniels, K. N. Kudin, M. C. Strain, O. Farkas, J. Tomasi, V. Barone, M. Cossi, R. Cammi, B. Mennucci, C. Pomelli, C. Adamo, S. Clifford, J. Ochterski, G. A. Petersson, P. Y. Ayala, Q. Cui, K. Morokuma, D. K. Malick, A. D. Rabuck, K. Raghavachari, J. B. Foresman, J. Cioslowski, J. V. Ortiz, A. G. Baboul, B. B. Stefanov, G. Liu, A. Liashenko, P. Piskorz, I. Komaromi, R. Gomperts, R. L. Martin, D. J. Fox, T. Keith, M. A. Al-Laham, C. Y. Peng, A. Nanayakkara, C. Gonzalez, M. Challacombe, P. M. W. Gill, B. Johnson, W. Chen, M. W. Wong, J. L. Andres, C. Gonzalez, M. Head-Gordon, E. S. Replogle, J. A. Pople, Gaussian 98, revision A.7 Gaussian, Inc., Pittsburgh, PA, **1998**.
- [26] J. H. Hardesty, J. B. Koerner, T. A. Albright, G.-Y. Lee, *J. Am. Chem. Soc.* **1999**, *121*, 6055.
- [27] F. H. Allen, J. E. Davies, J. J. Galloy, O. Johnson, O. Kennard, C. F. Macrae, E. M. Mitchell, G. F. Mitchell, J. M. Smith, D. G. Watson, *J. Chem. Inf. Comput. Sci.* **1991**, *31*, 187.
- [28] a) R. Hoffmann, *J. Chem. Phys.* **1963**, *39*, 1397; b) R. Hoffmann, W. N. Lipscomb, *J. Chem. Phys.* **1962**, *36*, 2179.
- [29] Examples of  $\eta^2$ -vinyl complexes as intermediates to allyl carbene complexes see: a) G. C. Canole, M. Green, M. McPartlin, C. Reeve, C. M. Woolhouse, *J. Chem. Soc. Chem. Commun.* **1988**, 1310; b) M. Green, M. F. Mahon, K. C. Molloy, C. B. M. Nation, C. M. Woolhouse, *J. Chem. Soc. Chem. Commun.* **1991**, 1587; c) S. J. Dossett, M. Green, M. F. Mahon, J. M. McInnes, J. M. J. Chem. Soc. Chem. Commun. **1995**, 767; d) R. J. Deeth, S. J. Dossett, M. Green, M. F. Mahon, S. J. Rumble, *J. Chem. Soc. Chem. Commun.* **1995**, 593; e) A. Fries, M. Green, M. F. Mahon, T. D. McGrath, C. B. M. Nation, A. P. Walker, C. M. Woolhouse, *Chem. Commun.* **1996**, 4517.
- [30] a) Y. Wakatsuki, N. Koga, H. Yamazaki, K. Morokuma, *J. Am. Chem. Soc.* **1994**, *116*, 8105; b) Y. Wakatsuki, N. Koga, H. Werner, K. Morokuma, *J. Am. Chem. Soc.* **1997**, *119*, 360; c) R. Stegmann, G. Frenking, *Organometallics* **1998**, *17*, 2089; d) C. Garcia-Yebra, C. Lopez-Mardomingo, M. Fajardo, A. Antinolo, A. Otero, A. Rodriguez, A. Vallat, D. Lucas, Y. Mugnier, J. J. Carbo, A. Lledos, C. Bo, *Organometallics* **2000**, *19*, 1749; e) N. Dölker, G. Frenking, *J. Organomet. Chem.* **2001**, *617–618*, 225; f) V. Cadierno, M. P. Gamasa, J. Gimeno, C. Gonzalez-Bernardo, E. Perez-Carreno, S. Garcia-Granda, *Organometallics* **2001**, *20*, 5177.
- [31] D. D. Perrin, W. L. F. Armarego, *Purification of Laboratory Chemicals*, 3rd ed., Pergamon, New York, **1988**.
- [32] a) M. Wildschek, C. Rieker, P. Jaitner, H. Schottenberger, K. E. Schwarzhans, *J. Organomet. Chem.* **1990**, *396*, 355; b) M. Buchmeiser, H. Schottenberger, *J. Organomet. Chem.* **1992**, *441*, 457; c) H. Schottenberger, J. Lukasser, E. Reichel, A. G. Müller, G. Steiner, H. Kopacka, K. Wurst, K. H. Ongania, K. Kirchner, *J. Organomet. Chem.* **2001**, *637–639*, 558, and references therein.
- [33] G. M. Sheldrick, SADABS: Program for Absorption Correction, University of Göttingen, Germany, **1996**.
- [34] G. M. Sheldrick, SHELXS97: Program for the Solution of Crystal Structures, University of Göttingen, Germany, **1997**.
- [35] G. M. Sheldrick, SHELXL97: Program for Crystal Structure Refinement, University of Göttingen, Germany, **1997**.
- [36] a) U. Haeusermann, M. Dolg, H. Stoll, H. Preuss, *Mol. Phys.* **1993**, *78*, 1211; b) W. Kuechle, M. Dolg, H. Stoll, H. Preuss, *J. Chem. Phys.* **1994**, *100*, 7535; c) T. Leininger, A. Nicklass, H. Stoll, M. Dolg, P. Schwerdtfeger, *J. Chem. Phys.* **1996**, *105*, 1052.
- [37] a) A. D. McClean, G. S. Chandler, *J. Chem. Phys.* **1980**, *72*, 5639; b) R. Krishnan, J. S. Binkley, R. Seeger, J. A. Pople, *J. Chem. Phys.* **1980**, *72*, 650; c) A. H. Wachters, *Chem. Phys.* **1970**, *52*, 1033; d) P. J. Hay, *J. Chem. Phys.* **1977**, *66*, 4377; e) K. Raghavachari, G. W. Trucks, *J. Chem. Phys.* **1989**, *91*, 1062; f) R. C. Binning, L. A. Curtiss, *J. Comput. Chem.* **1995**, *103*, 6104; g) M. P. McGrath, L. Radom, *J. Chem. Phys.* **1991**, *94*, 511.
- [38] a) J. E. Carpenter, F. Weinhold, *J. Mol. Struct. (Theochem)* **1988**, *169*, 41; b) J. E. Carpenter, *PhD thesis*, University of Wisconsin (Madison WI), **1987**; c) J. P. Foster, F. Weinhold, *J. Am. Chem. Soc.* **1980**, *102*, 7211; d) A. E. Reed, F. Weinhold, *J. Chem. Phys.* **1983**, *78*, 4066; e) A. E. Reed, F. Weinhold, *J. Chem. Phys.* **1983**, *78*, 1736; f) A. E. Reed, R. B. Weinstock, F. Weinhold, *J. Chem. Phys.* **1985**, *83*, 735; g) A. E. Reed, L. A. Curtiss, F. Weinhold, *Chem. Rev.* **1988**, *88*, 899; h) F. Weinhold, J. E. Carpenter, *The Structure of Small Molecules and Ions*, Plenum, **1988**, 227.
- [39] K. B. Wiberg, *Tetrahedron* **1968**, *24*, 1083.

Received: February 14, 2002 [F3875]